JOC The Journal of Organic Chemistry

Article

pubs.acs.org/joc

Stereoselective Wittig Olefination as a Macrocyclization Tool. Synthesis of Large Carbazolophanes

Damian Myśliwiec, Tadeusz Lis, Janusz Gregoliński, and Marcin Stępień*

Wydział Chemii, Uniwersytet Wrocławski, ul. F. Joliot-Curie 14, 50-383 Wrocław, Poland

Supporting Information

ABSTRACT: *Z*-Selective Wittig olefination was applied to the synthesis of large carbazolophanes containing up to eight heteroaromatic subunits. A number of strategies were devised and tested, showing that cyclooligomerization yields can be significantly improved by using one-component schemes involving heterobifunctional reactants. [4]- and [6]-Carbazolophanes were characterized in the solid state, revealing compact, highly folded structures. Electronic and steric effects of substitution and chain length on the Wittig olefination rates and *Z*-selectivities were explored theoretically using DFT calculations.

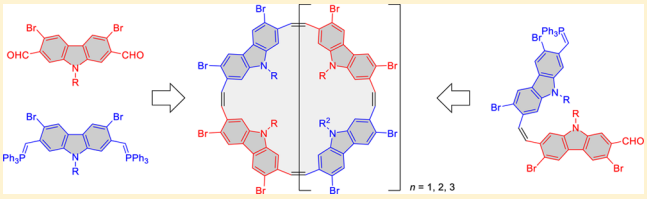

INTRODUCTION

One of the most important approaches to the synthesis of artificial macrocyclic structures is cyclooligomerization of small molecule precursors.[1−3] In such syntheses, one or more bifunctional substrates are typically reacted under high-dilution conditions, to yield product mixtures that contain varying amounts of macrocycles. Because of its simplicity, this methodology can provide rapid access to complicated target molecules, which are usable as supramolecular building blocks and parts of molecular machinery. Many important classes of macrocyclic systems are available through this general strategy, including cyclophanes,[4] cycloparaphenylenes,[5−7] calixarenes,[8] cucurbiturils,[9] pillararene-like systems,[10,11] and pyrrole-based macrocycles.[12,13]

The principal limitations of cyclooligomerization reactions are associated with their usually moderate chemical yields and often imperfect ring-size selectivity. These problems can often be obviated, sometimes in a spectacular fashion, by employing removable templates of varying shapes and sizes[14−21] or through the use of intramolecular templating effects, e.g., those based on hydrogen bonding.[22,23] In the absence of a templating effect, the efficiency of cyclooligomerization is usually limited, especially with regard to higher cyclo-*n*-mers (e.g., $n > 4$), which are usually obtained in minute yields and may be difficult to isolate.[24−28] Product distribution and overall yields heavily depend on the reaction type and structure of precursors in a manner that is difficult to predict. Because of the step-growth nature of the oligomerization process,[29] the chain length can quickly exceed the range suitable for macrocyclization,[1] leading to the formation of unwanted polymers. Consequently, highest yields and selectivities are typically observed for thermodynamically controlled reactions, which benefit from their "self-correcting" ability.[1,30] Nevertheless, kinetically controlled cyclooligomerizations can take advantage of many useful but inherently irreversible reaction types[24] (e.g., Williamson etherification, metal-catalyzed couplings). Such reactions are better suited for high-dilution techniques and are more easily transformed into stepwise synthetic schemes. Stepwise strategies not only help improve ring-size selectivity but also provide access to unsymmetrically substituted derivatives.

In the context of the above discussion, the Wittig olefination reaction might seem a particularly attractive cycloligomerization method because it is mechanistically well understood and capable of providing high chemical yields.[31−33] Furthermore, being an irreversible process, the Wittig reaction should be amenable to the high dilution technique, which is most reliable under perfect kinetic control. Indeed, the Wittig olefination was employed for the synthesis of structurally diverse macrocycles, most notably cyclophanes[34−55] and naturally occurring bisbibenzyls.[56] In contrast to direct cyclizations, which provide an efficient route to moderately sized rings, reported Wittig cyclooligomerizations were usually low-yielding (typical yields below 20%) and, in many instances, yields of 1−2% were considered publishable. To date, no systematic study of the Wittig cyclooligomerization has been performed, and the reasons for its limited efficiency are not fully understood. It can be hypothesized that the principal problem lies in the unfavorable combination of limited *Z*/*E*-stereoselectivity, associated with the prevalent use of semistabilized arylmethylene ylides, and the step-growth nature of the oligomerization process. Furthermore, in the case of completely unsaturated reactants, partial conformational restriction of the growing oligoalkene chain might result in low cyclization probabilities. The situation can be further complicated by various side reactions, to which phosphorus ylides are susceptible, such as hydrolysis[57,58] or homocoupling.[59] Finally,

Received: April 4, 2015
Published: May 14, 2015

DOI: 10.1021/acs.joc.5b00745
J. Org. Chem. 2015, 80, 6300−6312

large macrocycles containing multiple double bonds may form as complex mixtures of stereoisomers with limited configurational stability, leading to isolation and characterization problems.

In contrast to the typical behavior observed for semistabilized ylides, arylmethylene phosphoranes react with many ortho-substituted aromatic aldehydes, yielding predominantly (*Z*)-stilbenes, and this anomalous stereoselectivity is further enhanced by ortho-substitution on the ylidic aryl group.[33,60−64] To date, direct cyclooligomerizations employing ortho-substituted reactants have not been attempted, even though increased *Z*-selectivity of consecutive olefination steps could be beneficial for the overall macrocyclization efficiency. In the recently reported "fold-in" synthesis of chrysaorole[65,66] (**4a**, Scheme 1), we have employed a double *Z*-selective Wittig

Scheme 1. Synthesis of Chrysaorole (4a)[65]

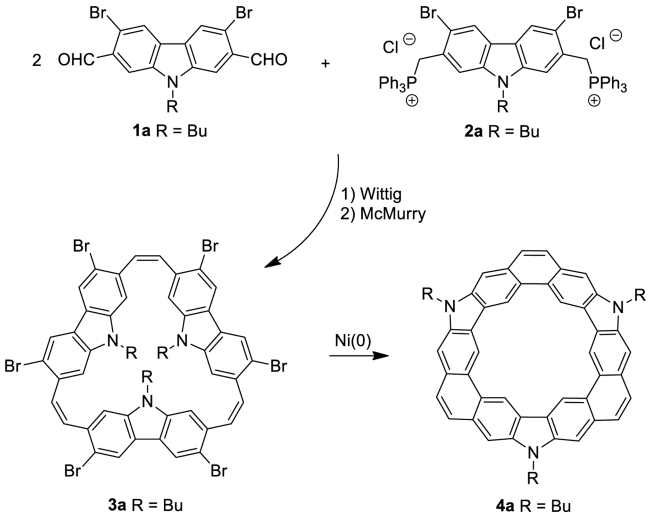

olefination reaction between dialdehyde **1a** and the diylide derived from the salt **2a**, which enabled a high yielding and ring-size selective synthesis of carbazolophane **3a**. Here we develop a modular cyclooligomerization protocol based on the stereoselective Wittig coupling of functionalized carbazoles. The protocol provides access to macrocycles with varying substitution patterns and ring sizes (up to 72-membered). In the context of these experimental results and with the help of high level quantum chemical calculations, we develop a kinetic model which probes the relationship between cyclooligomerization yields and relative end group reactivities.

RESULTS AND DISCUSSION

Cyclooligomerization of Monocarbazoles. The simplest and most frequently used macrocyclization protocol based on the Wittig olefination is the two-component reaction between a dialdehyde and a diylide.[34,37−54] It can be contrasted with one-component routes, which require heterobifunctional reactants (aldehyde-ylides) that are typically less convenient to prepare.[35,36,46,55,56] In the following discussion two- and one-component routes will be designated C*n*C + P*m*P and C*n*P, respectively, where *n*, *m* > 0 denote the number of carbazole units in the oligomer chain. Thus, **C1C + P1P** will refer to the two-component reaction between monocarbazoles. The prototypical reaction of this kind was carried out between dialdehyde **1a** and diphosphonium salt **2a**, affording a mixture of (Z^4)-[2_4](2,7)carbazolophanetetraene **5a**, (Z^5E)-[2_6](2,7)-carbazolophanehexaene **6a**, and additional unidentifiable oligomeric products (Scheme 2). The synthesis was most

Scheme 2. Two-Component Wittig Cyclooligomerization of Monocarbazoles[a]

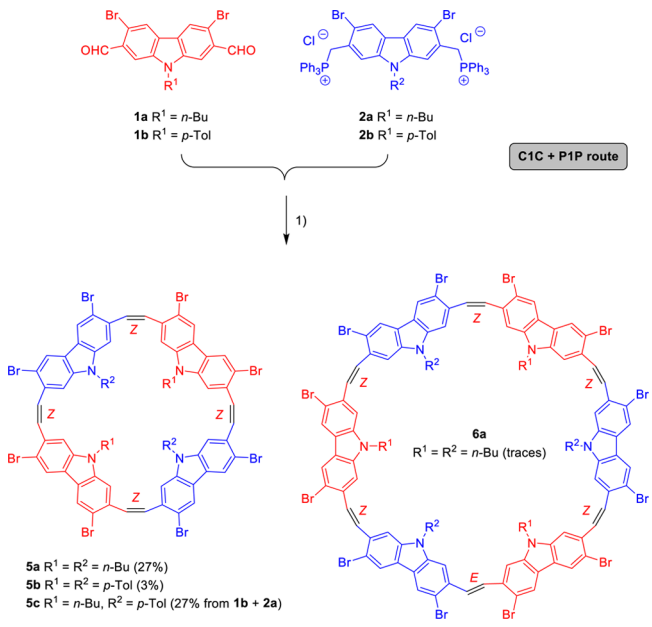

[a]Reagents and conditions: (1) NaOH (50%), dichloromethane, 1.6 mM reactant concentration.

conveniently carried out in dichloromethane (1.6 mM reactant concentrations), using 50% aqueous NaOH as the catalyst. However, other typical reaction conditions (DBU in dichloromethane, *t*-BuOK in DMF) were also found to be efficient. **5a** was separated from the reaction mixture by means of column chromatography and isolated in 27% yield after crystallization. The stability of **6a** in solution was limited, and the compound decomposed during prolonged chromatography on silica or alumina columns. The decomposition apparently includes but is not limited to the isomerization of vinylene bridges. Effective purification of **6a** was only achieved by means of gel permeation chromatography. Because of the instability of **6a** and some of the linear oligocarbazoles discussed below, it was advantageous to determine reaction yields (and stereoisomer ratios) on the basis of careful integration of ^{1}H NMR spectra of crude reaction mixtures. The integrations were performed relative to signals of triphenylphosphine oxide, which is a convenient reference because it is formed stoichiometrically in the Wittig reaction and in the accompanying ylide hydrolysis.[58] Isolated yields for configurationally stable products were in good agreement with NMR data.

The scope of the reaction was expanded by employing *p*-tolyl-substituted dialdehyde **1b** and diphosphonium salt **2b**. The Wittig condensation of these two compounds furnished the tolyl-substituted cyclotetramer **5b** in only 3% yield as the sole macrocyclic product. The low efficiency of the latter synthesis is likely caused by steric effects, as discussed below. In contrast, the reaction between **1b** and **2a** produced the mixed product **5c** in comparable yield to that of **5a** (27%). Larger macrocycles apparently form alongside **5c**, but they resisted our isolation attempts and their structures could not be inferred from the NMR spectra of crude mixtures.

DOI: 10.1021/acs.joc.5b00745
J. Org. Chem. 2015, 80, 6300−6312

Even though cyclodimers could potentially be formed in the two-component Wittig macrocyclization, no such products have been observed in any of the reactions described above. In contrast, the McMurry cyclooligomerization of **1a** produced cyclodimer **7a** (18%) and cyclotrimer **3a** (8%[65]) as the principal nonpolymeric products (Scheme 3). The solid-state

Scheme 3. Synthetic Chemistry of Carbazole Cyclodimers[a]

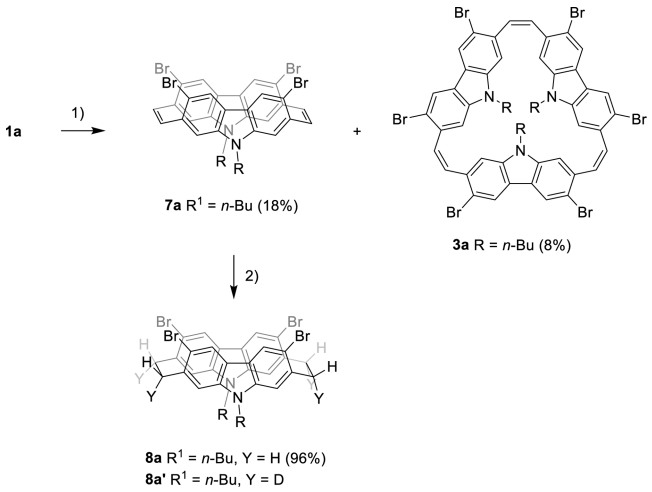

[a]Reagents and conditions: (1) $TiCl_4$, Zn, CuI, THF, reflux, slow addition. (2) *p*-$TsNHNH_2$, AcONa, DCM, H_2O or D_2O.

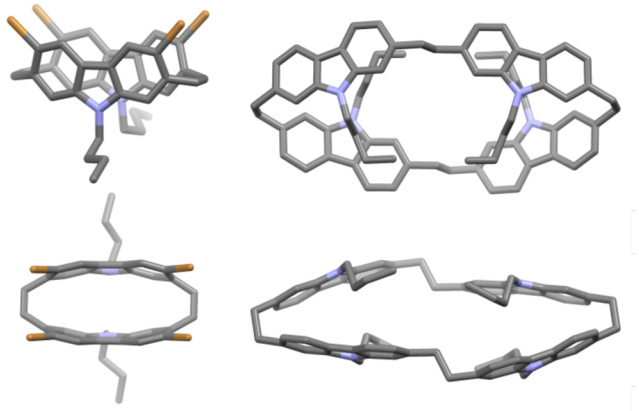

Figure 1. Molecular geometries of **7a** (left) and **16a** (right) determined in X-ray crystallographic analyses. Hydrogen atoms, additional symmetry independent molecules, and disordered groups are removed for clarity.

structure of **7a** (Figure 1) revealed that this compound is formed selectively in the syn configuration (i.e., with both nitrogen atoms on the same side of the macrocycle). DFT calculations indicate that the hypothetical anti structure of **7a** has a higher energy than the syn isomer, suggesting that the observed stereoselectivity of cyclization is inherent to the mechanism of the McMurry coupling. The bending of carbazole subunits, characteristic of small cyclophane rings, indicates that considerable internal strain is present in the molecule of **7a**. The π-electron conjugation in this macrocycle is apparently diminished by the near orthogonal arrangement of vinylene bridges relative to carbazole rings. Consequently, the yellow color characteristic of the higher cyclooligomers is much weaker in **7a**.

Structure and Properties of Cyclooligomers. X-ray crystallographic analyses of carbazolophanes **5a–c** show that in the solid state, all three macrocycles adopt similar conformations characterized by the alternating up-and-down arrangement of N-substituents (Figure 2). In each case, the macrocycle

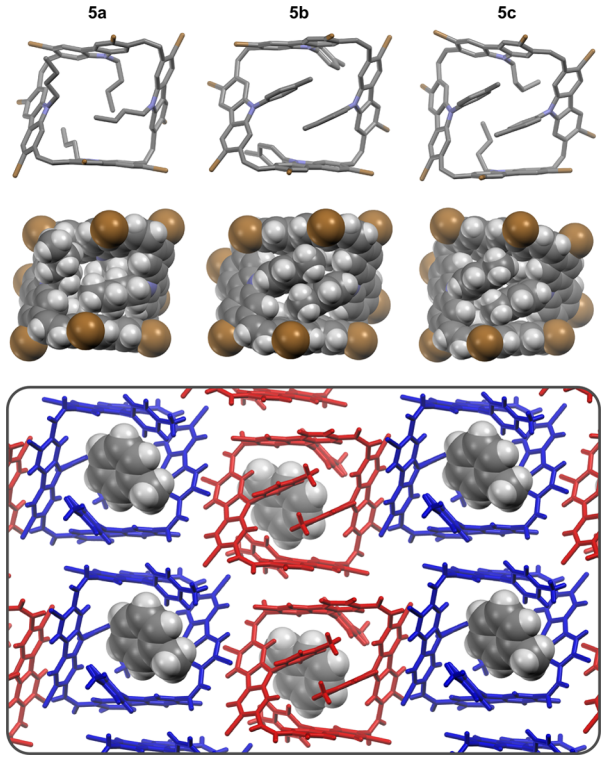

Figure 2. Top: molecular structures of carbazolophanes **5a–c** observed in the solid state. Solvent molecules, disordered butyl chains, and hydrogen atoms (in the stick model) are omitted for clarity. Bottom: 2D layer packing of **5b** showing partial encapsulation of toluene molecules. Additional toluene molecules located between layers are not shown. Molecules related by a primitive translation have the same color.

is twisted and folded to form a relatively compact structure with an interior tightly packed with the substituent groups. In **5b**, two of the *p*-tolyl substituents form a laterally shifted van der Waals contact, effectively closing the macrocyclic core on one side. The macrocycle opens on the other side, forming a cavity that is ca. 4 Å deep and is occupied by a toluene molecule in the solid-state structure. In the crystal, molecules of **5b** form layers that are stabilized in two dimensions by π-stacking interactions between neighboring carbazole fragments, and to a lesser extent by Br···Br interactions (Figure 2). A similar packing pattern is observed in the structure of **5a**, whereas **5c** shows the π-stacking aggregation only in one dimension (Figure S9, Supporting Information). In the above structures some of the $\pi-\pi$ contacts are "slipped", but the interacting aromatic planes are roughly parallel.

The ^{1}H NMR spectra of compounds **5a–c** reflect the symmetry of their respective substitution patterns and are consistent with the structures derived from diffraction analyses. In **5a** and **5c**, signals of butyl substituents show upfield relocations relative to typical values indicating shielding effect of the neighboring carbazole moieities (e.g., CH_3 protons

DOI: 10.1021/acs.joc.5b00745
J. Org. Chem. 2015, 80, 6300–6312

resonate at 0.30 and 0.27 ppm in **5a** and **5c**, respectively). At room temperature, the ortho and meta protons of the *p*-tolyl groups in **5b** and **5c** are significantly broadened. This broadening, corresponding to the fast exchange limit, is consistent with the pairwise inequivalence of ortho and meta protons in each tolyl substituent. The differentiation of the ortho and meta signals is expected in a rigid folded conformation of the macrocycle, similar to the solid-state geometry. Partial coalescence observed at room temperature can be explained in terms of substituent rotation around the C−N bond. Alternatively, the macrocycle might undergo rapid pseudoinversion, but this process is expected to be hindered by the rigid and bulky tolyl substituents.

In the solid state, cyclohexamer **6a** adopts a butterfly shaped conformation, in which the N-substituents alternate above and below the mean plane of vinylene bridges, as seen earlier in the structures of cyclotetramers (Figure 3). The two carbazole moieties adjacent to the unique (*E*)-vinylene bridge are roughly coplanar, and the molecule is folded in such a way that the (*E*)-vinylene fragment lies within a van der Waals contact distance from the topologically most remote (*Z*)-vinylene bridge. In the crystal, the macrocyclic skeleton loosely approximates the C_2 point symmetry, with the symmetry axis passing through the (*E*)-vinylene bond. Four butyl substituents are directed toward the interior of the macrocycle, whereas the remaining two chains are located in the outer "bay". As a result, the molecule forms a trapezoidal block with three of its faces occupied by π-aromatic surfaces. In the solid state, molecules of **6a** form centrosymmetric dimers interacting via the longest π-aromatic face, which contains the (*E*)-vinylene bond. These dimeric aggregates are further arranged into layers (Figure 3C), which are organized along the shorter π-aromatic edges containing single carbazole units. The carbazole surfaces are roughly perpendicular to the packing plane and parallel between consecutive molecules. However, the corresponding interactions have limited $\pi-\pi$ stacking character because of the large parallel displacement between the adjoining carbazole fragments.

The ^{1}H NMR spectrum of **6a**, recorded in chloroform-*d* at 250 K, contains 12 carbazole signals, indicative of a structure with 2-fold symmetry (Figure 4). Additionally, 6 vinylene signals are observed, including two near-degenerate AB spin systems (at 6.87 and 6.89 ppm) and two singlets at 6.73 and 7.65 ppm. The overlapping multiplets in the upfield region of the spectrum correspond to three nonequivalent pairs of butyl chains. The α-CH_2 signals of the butyl groups show marked diastereotopicity, which is consistent with either C_2 or C_s point symmetry of the molecule. Signals of CH_3 groups (0.00 to −0.56 ppm) resonate upfield relative to typical shift values observed in *N*-butyl carbazoles (ca. 0.9 ppm), indicating a shielding effect of the neighboring aromatic groups. On the basis of scalar and dipolar correlations observed in the COSY and ROESY spectra, it was possible to establish the connectivity among the consecutive carbazole subunits and vinylene bridges. In addition, the ROESY spectrum reveals a number of nontrivial through-space contacts (Figure 4, right) between topologically distant protons in the molecule. These contacts show that the butterfly conformation observed in the solid state is preserved in solution. In particular, a strong correlation between the two vinylene singlets at 6.73 and 7.65 ppm was identified, corresponding to the transannular contact involving the (*E*)-vinylene bridge. The unique pattern of ROE correlations between butyl and carbazole signals (Figure 4, right) indicates that the preferred orientation of alkyl chains resembles that observed in the solid state.

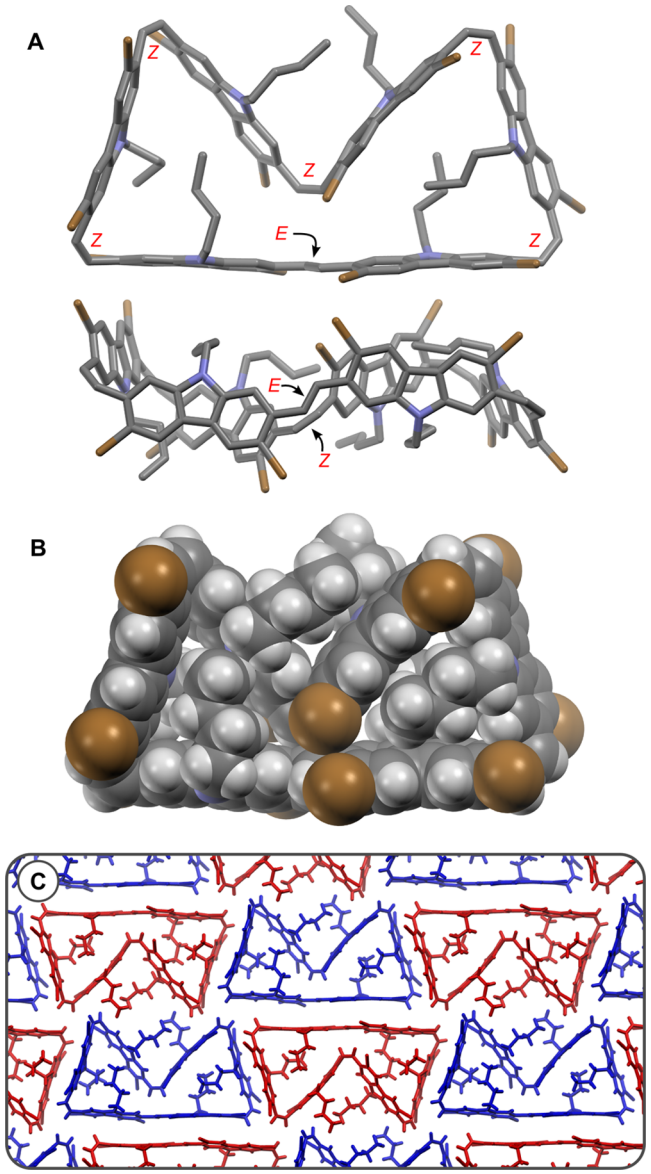

Figure 3. Molecular structure of carbazolophane **6a** observed in the solid state. The disorder of butyl substituents is not shown. (A) Stick diagram showing the positions of double bond linkages. (B) van der Waals diagram showing the internal packing of substituents. (C) Packing diagram. Molecules related by a primitive translation have the same color.

At temperatures above 250 K, the diastereotopic methylene signals of the butyl chains undergo gradual broadening and partial coalescence. The latter change may be thought to indicate that the chiral C_2-symmetric conformation of **6a** is not completely rigid and undergoes a pseudoinversion in solution. The carbazole and vinylene peaks do not broaden at higher temperatures, indicating that the (*E*)-vinylene bond does not migrate. The inversion of **6a** is potentially a complex process, possibly occurring via stepwise rotation of carbazole subunits in the macrocyclic frame. In addition to dynamic broadening, changes of the temperature induce small variations of chemical shifts, which are likely associated with a temperature-dependent conformational equilibrium.

DOI: 10.1021/acs.joc.5b00745
J. Org. Chem. 2015, 80, 6300−6312

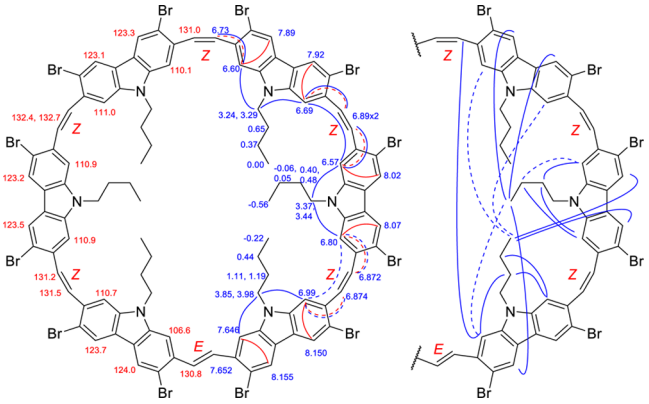

Figure 4. Assignment of signals in the ^{1}H and ^{13}C NMR spectra of **6a** (excluding quaternary carbons) obtained on the basis of $^{1}H-^{1}H$ COSY and ROESY correlations (red and blue lines, respectively), and a $^{1}H-^{13}C$ HSQC spectrum. ^{1}H and ^{13}C chemical shifts are indicated respectively as blue and red labels.

Alternative Synthetic Pathways. The viable formation of linear carbazole oligomers via the Wittig protocol, initially explored in the chrysaorole synthesis,[65] indicated their possible use as precursors to larger cyclophane macrocycles. Tricarbazoles with two terminal aldehyde (**12a**),[65] chloromethyl (**10a**), and phosphonium (**11a**) groups were prepared with good though not perfect (*Z*)-stereostelectivities, as shown in Scheme 4. The *ZZ* configuration of the principal isomers was

Scheme 4. Synthesis of Linear Tricarbazoles[a]

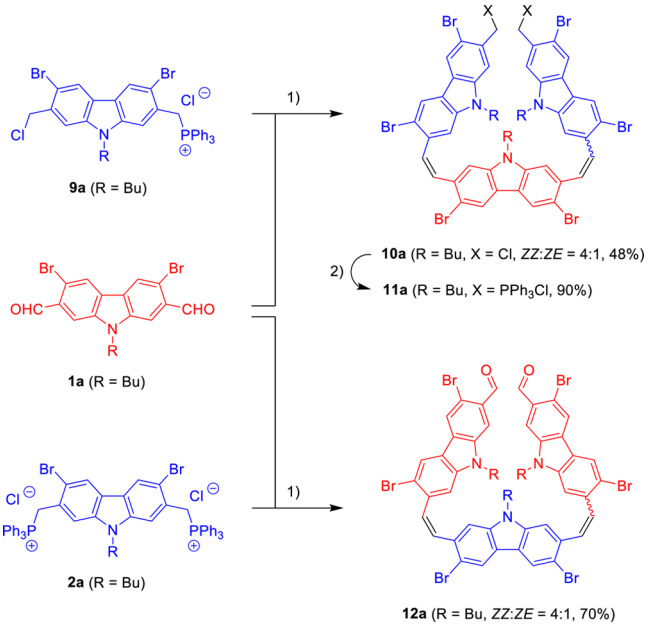

[a]Reagents and conditions: (1) aq NaOH, dichloromethane; (2) PPh_3, toluene, 150 °C, pressure tube. Reactant ratios: **1a**:**9a** = 1:3, **1a**:**2a** = 4:1.

determined on the basis of the vinylene ^{3}J couplings observed in the ^{1}H NMR spectra and further confirmed for (*ZZ*)-**10a** in an X-ray crystallographic analysis (Supporting Information). Because of separation problems, isomeric mixtures of **11a** and **12a** were used in subsequent Wittig cyclooligomerization experiments. To test an alternative synthetic route to cyclotetramers (labeled P3P + C1C in Scheme 5), the

Scheme 5. Two-Component Macrocyclizations Involving Tricarbazole Building Blocks (the position of the *E* bond in 6a relative to the color-coded halves of the molecule is arbitrary)

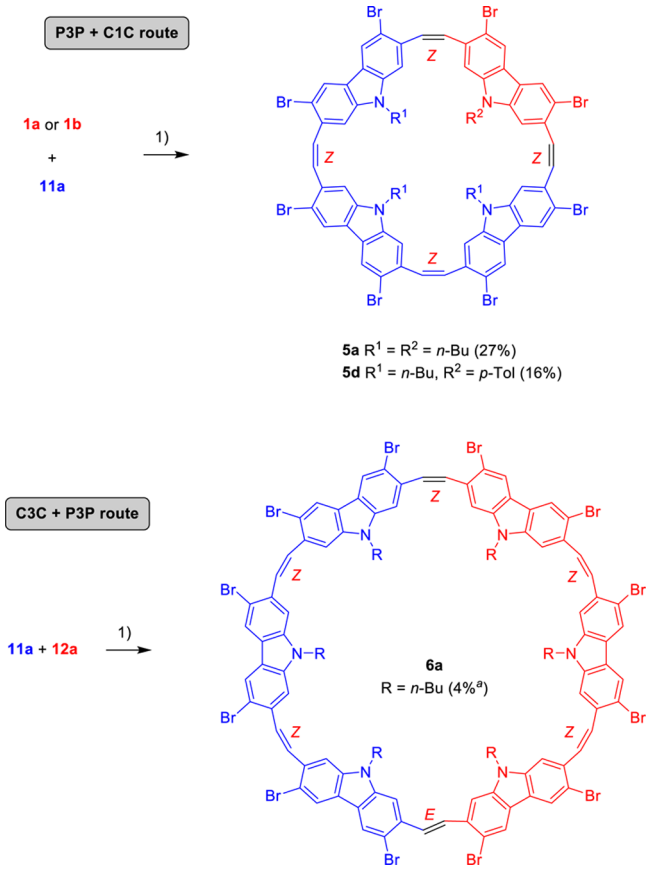

[a]Yield determined by NMR integration.

diphosphonium salt **11a** was reacted with aldehydes **1a** and **1b**, producing cyclotetramers **5a** and **5d**, respectively. The latter compound possesses an unsymmetrical substitution pattern, which cannot be selectively obtained by cyclooligomerization of monocarbazoles. The P3P + C1C route should formally be selective toward macrocycles containing 4*n* subunits, and indeed, cyclohexamer **6a** did not form in the reaction between **11a** and **1a**.

The C3C + P3P route (Scheme 5), involving two tricarbazole reactants, was thought to provide an analogous selectivity toward 6*n* macrocycles. Hexamer **6a** indeed formed selectively in the reaction between **11a** and **12a** (no **5a** was observed), but the yield was still low (ca. 4% by NMR). It should be noted here that the unique *E* vinylene bridge in **6a** can be formed during the chain growth stage at one of three nonequivalent positions in the linear hexamer chain (*EZZZZ*-, *ZEZZZ*-, and *ZZEZZ*-C6P), or it can alternatively be produced from Z^6-C6P in the macrocycle-closing step. Overall, four different ring closure pathways can be envisaged, which may significantly differ in their respective cyclization probabilities. The C3C + P3P route increases the relative abundance of linear hexamers in the reaction mixture, in comparison with the C1C + P1P approach, but it is also likely to affect the isomer distribution of the C6P chain. The outcome of the latter change cannot be predicted in such a complex reaction, but its effect on **6a** yields is not necessarily positive.

DOI: 10.1021/acs.joc.5b00745
J. Org. Chem. 2015, 80, 6300−6312

Scheme 6. C2P Cyclooligomerization Route[c]

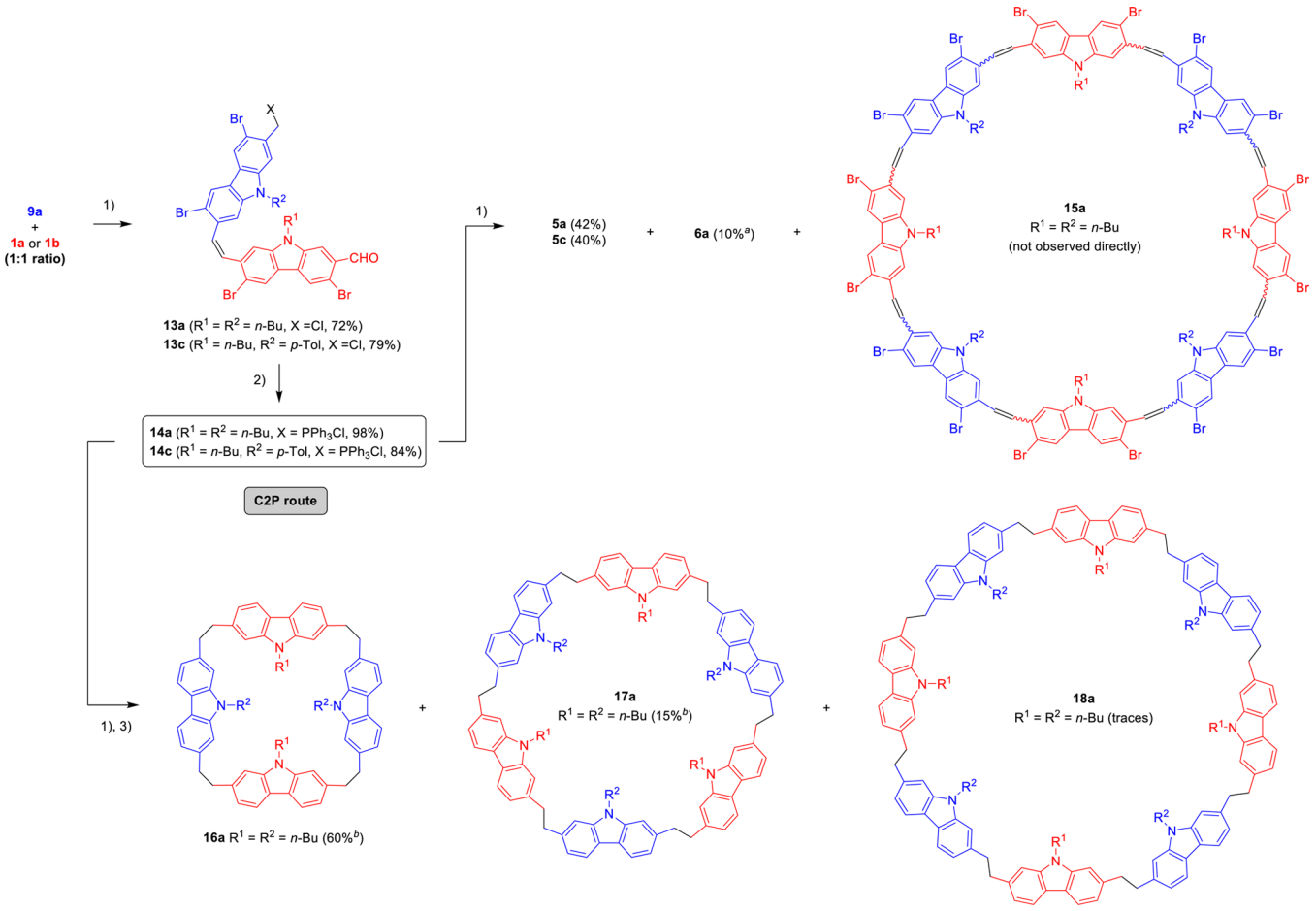

[a]Yield by NMR integration [b]Hydrogenation yield. [c]Reagents and conditions: (1) 50% NaOH(aq), DCM; (2) PPh_3, benzene, 90 °C; (3) H_2, Pd/C.

All of the above synthetic routes were of the two-component type, i.e., involving two homobifunctional reactants (dialdehyde and diylide). These syntheses are complemented by the one-component approach, in which a formyl-phosphonium salt acts as the sole cyclooligomerization precursor. Dicarbazole salts **14a** and **14c** were conveniently prepared by means of condensing **9a** with dialdehydes **1a** and **1b**, respectively, and reacting the resulting intermediates **13a** and **13c** with triphenylphosphine (Scheme 6). **14a** was subjected to the one-component Wittig cyclooligomerization (C2P route), providing the expected cyclotetramer **5a** and cyclohexamer **6a** in significantly improved yields (42% and 10%, Scheme 6). A similar improvement was observed for **5c** (40%).

Hydrogenation Experiments. Despite the high *Z*-selectivity of a single Wittig olefination step, *E* double bonds will form to some extent in both cyclic and linear products, either directly in the disfavored *E*-selective route or in the course of subsequent isomerization. Hydrogenation of crude macrocycle mixtures was attempted as a possible means of removing the source of stereoisomerism associated with vinylene linkages. Diimide reductions performed on cyclooligomer mixtures under a variety of reaction conditions were either inefficient or led to unidentifiable products with unexpectedly high polarity. In striking contrast, cyclodimer **7a** was cleanly hydrogenated to **8a** using *p*-tosyl hydrazide under basic conditions (Scheme 3). The use of sodium acetate/deuterium oxide as the base source led to the stereoselective formation of the deuterated derivative **8a′**. On the basis of a ROESY spectrum recorded for **8a**, it was verified that the hydrogens are transferred from the diimide to the less encumbered side of the double bond in **7a** (away from the bromine atoms). This result suggests that, for larger macrocycles, the low efficiency of hydrogenation may be associated with the geometrical factors around the double bond, in particular with the spatial arrangement of bromine atoms.

In contrast to diimide reductions, catalytic hydrogenations were capable of completely reducing double bonds in larger cyclooligomers. However, the process was invariably associated with considerable reductive debromination, even in the presence of potentially more selective catalysts (e.g., PtO_2/$NaNO_2$). Interestingly, an exhaustive hydrogenation−dehydrohalogenation of the cyclooligomers was possible under 1 atm H_2 when palladium on activated carbon was used as the catalyst. Upon hydrogenation of the **14a** cyclooligomerization products, the mixture was found to comprise the reduced cyclic oligomers **16a**, **17a**, and **18a**, containing respectively four, six, and eight carbazole subunits (Scheme 6). These compounds were identified on the basis of their highly symmetric ^{1}H NMR spectra, the relative diffusion coefficients determined using diffusion-ordered spectroscopy (DOSY, Figure S10, Supporting Information), and mass spectrometric analyses. In the crude mixture, **16a**, **17a**, and **18a** were observed in a 1:0.4:0.1 molar ratio, and the first two compounds were isolated in 60% and 15% yield, respectively. The presence of **18a** in the hydro-

DOI: 10.1021/acs.joc.5b00745
J. Org. Chem. 2015, 80, 6300−6312

genated mixtures implies that the crude Wittig product contained, in addition to **5a** and **6a**, also the corresponding cyclooctamer **15a**. The latter species is likely to form as a mixture of stereoisomers and was not directly identifiable in the crude cyclooligomerization mixtures prior to hydrogenation.

Computational Analysis of the Wittig Olefination. High-level DFT calculations have recently been shown to provide valuable insight into the mechanism of the Wittig olefination reaction.[67−69,64] It was found that relative transition-state energies could be estimated with sufficient precision to enable semiquantitative predictions of reactivity in differently stabilized ylides.[67,68] In the case of substituted (benzylidene)-triphenylphosphoranes, such as those derived from **2**, DFT calculations were used to rationalize the anomalous stereoselectivity induced by ortho-substitution of aldehydes and correctly reproduced the linear free-energy relationships between aldehyde and ylide substitution and olefination rates.[64] The latter capability is of direct relevance to the present work because it can be used to discover reactivity patterns operating at consecutive stages of oligomerization. To probe the effect of remote substitution on a single olefination step, the geometry of the *Z*-selective transition-state TS1 was optimized for several pairs of mono- and dicarbazole reactants (Scheme 7, Table 1, Figure 5). To simplify the conformational space, the *N*-alkyl groups present in the actual reactants were replaced with hydrogens in the model structures. It was assumed that the electronic effects of the N-substituent are similar of all reaction studied and will have a negligible effect on the relative reaction rates. The geometry of *Z*-TS1 previously reported for the 2-bromobenzaldehyde/(2-bromobenzylidene)-triphenylphosphane pair[64] was used to construct the initial geometries for transition-state optimization.

Scheme 7. *Z*-Selective Wittig Olefination between Two Carbazole Reactants, Modeled Using DFT Methods[a]

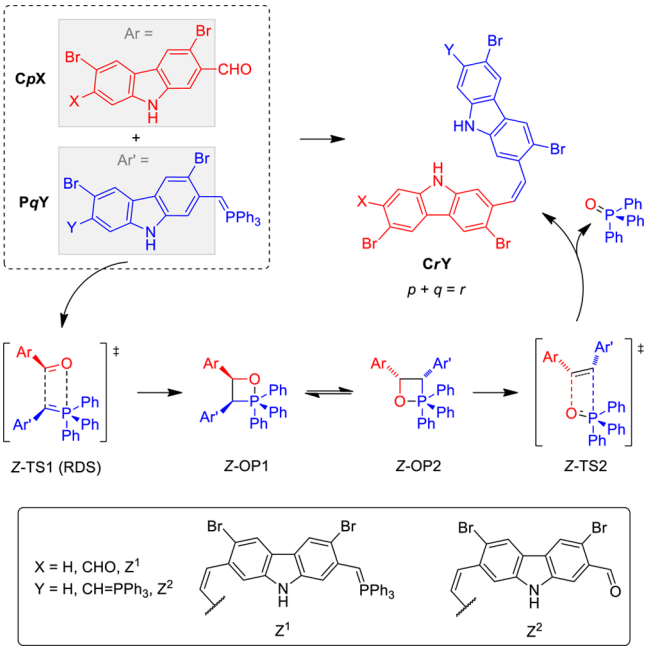

[a]Key steps of the currently accepted mechanism[33] are indicated (TS, transition state; OP, oxaphosphetane; RDS, rate-determining step). **C2P** is the preferred designation to **P2C**.

Table 1. Calculated Relative Activation Energies and Reaction Rates for Model Wittig Olefinations

reaction	X[a]	Y[a]	$\Delta\Delta E^{\ddagger}$[b]	k_{XY}/k_{HH}[c]
C1C + P1P → C2P	CHO	$CH{=}PPh_3$	−2.76	117.4
C1C + P1H → C2H	CHO	H	−1.29	9.3
C1H + P1P → H2P	H	$CH{=}PPh_3$	−1.41	11.4
C1H + P1H → H2H	H	H	0.00	1.0
C1C + C2P → C3C	CHO	Z[2d]	−0.86	4.4
C2P + P1P → P3P	Z[1d]	$CH{=}PPh_3$	−1.38	10.8
C2P + C2P → C4P	Z[1d]	Z[2d]	0.31	0.58

[a]X and Y substituents as defined in Scheme 7. [b]Activation energy (B3LYP/6-31G(d,p)/PCM(CH_2Cl_2), kcal/mol) calculated for the *Z*-selective TS1 relative to the unsubstituted reactant pair (X = Y = H). [c]Relative reaction rates calculated from $\Delta\Delta E^{\ddagger}$. [d]Substituents defined in Scheme 7.

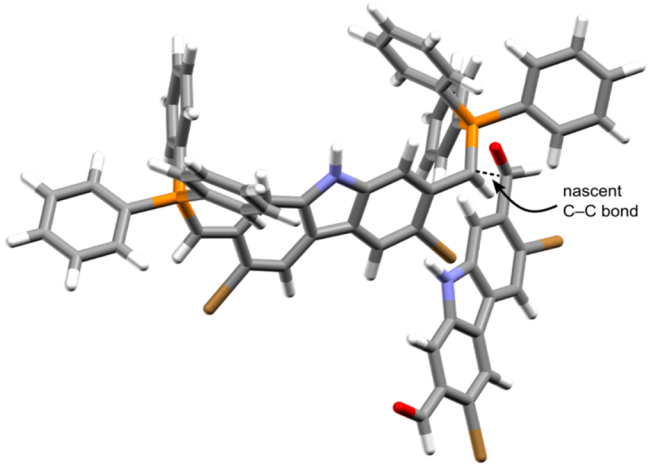

Figure 5. Optimized *Z*-TS_1 geometry for the **C1C + P1P** reaction.

The relative reaction rate constants k_{XY}/k_{HH} predicted for different reactant pairs (Table 1) cover approximately 3 orders of magnitude. The accelerating effect of electron-withdrawing groups on the aldehyde reactant[70,60,71] can be seen in additions involving **C1C**, which are ca. 10 times faster than the corresponding reactions of **C1H**. A comparable rate enhancement resulting from ylide substitution[64] is predicted for the **P1P** diylide, indicating that the additional $CH{=}PPh_3$ group acts as an electron-donating substituent. The activating effects of aldehyde and ylide substitutuents are cumulative, and consequently, the **C1C + P1P** reaction is predicted to be particularly fast. In the reaction with **P1P**, the aldehyde group of **C2P** shows comparable reactivity to that in **C1H**. In contrast, the ylide function in **C2P** is moderately deactivated relative to the **P1H** ylide group, as evidenced by the calculated rate constants for **C1C + C2P** and **C2P + C2P** additions. Data in Table 1 indicate that the end group effects on rate constants are rapidly attenuated with the increasing length of oligocarbazole chains and will be kinetically relevant only for steps involving monocarbazole species. Still, in the course of Wittig oligomerization, one can expect three distinct ranges of rate constants, corresponding to (1) **C1C + P1P**, (2) **C1C + P*n*P** or **C*m*C + P1P**, and (3) **C*m*C + P*n*P** ($m, n > 1$), with a predicted ratio of ca. 100:10:1. It should be noted, however, that in different reactant systems, e.g., based on *p*-phenylene derivatives, the end group effects would likely be stronger and could propagate efficiently over longer oligomer chains. Preliminary kinetic modeling, using a variant of the model

DOI: 10.1021/acs.joc.5b00745
J. Org. Chem. 2015, 80, 6300−6312

developed by Ercolani, Mandolini, and Mencarelli,[72] showed that such differentiation of k values can have an influence on cyclization yields and product distribution in cyclooligomerization reactions. The effect is particularly evident in C1C + P1P routes (because of the strong inductive effects) and is predicted to lead to a decrease in cyclization yields, in comparison with one-component cyclooligomerizations, in line with experimental observations.

The high Z-selectivity observed experimentally in the synthetic work described above is reproduced by DFT calculations. For the **C1C** + **P1P** reaction, the energy difference between the Z- and E-selective TS1 is $\Delta E^{\ddagger}(Z\text{-TS1}) - \Delta E^{\ddagger}(E\text{-TS1}) = -2.60$ kcal/mol, corresponding to a rate constant ratio k_Z/k_E of ca. 89. This value is nearly identical to that reported previously for the model reaction between *o*-bromobenzaldehyde and (*o*-bromobenzylidene)triphenylphosphorane (−2.61 kcal/mol),[64] indicating that the Z-selectivity is principally governed by the steric ortho-effects and is not significantly affected by the electronic effects of remote functionalization or ring fusion. It might thus be reasonable to expect that the k_Z/k_E ratio is likely to be similar also for higher oligomerization steps. However, the TS geometry shown in Figure 5 reveals that a sufficiently large and rigid N-substituent bound to the **C1C** dialdehyde may interfere sterically with the remote triphenylphosphorane group of **P1P**. No such interference is predicted for the corresponding E-TS1 geometry, indicating that the Z-selectivity may be affected by remote steric effects, thus compromising yields of all-Z macrocycles and linear oligomers. The uniquely low yield of **5b** in the **C1C** + **P1P** synthesis may be one of the indications of this effect.

CONCLUSIONS

With sufficiently high stereoselectivity, the Wittig olefination provides a viable cyclooligomerization protocol capable of producing uniquely large cyclophane structures. Functionalized cyclophanes available from the present protocol, such as the carbazole-containing structures presented herein, are prospective precursors to highly fused heteroaromatic systems. The irreversible character of the Wittig reaction enables stepwise elaboration of unsymmetrically substituted macrocycles. The present work sheds new light on the synthetic limitations of the Wittig-based cyclooligomerization strategies and shows how the cyclization yields can be improved by appropriate precursor design and selection of synthetic routes. Further refinements of the present approach are currently under investigation.

EXPERIMENTAL SECTION

General. Tetrahydrofuran, toluene, and *N*,*N*-dimethylformamide were dried using a commercial solvent purification system. Dichloromethane was distilled from calcium hydride when used as a reaction solvent. ^{1}H NMR spectra were recorded on high-field spectrometers (^{1}H frequency 500.13 or 600.13 MHz), equipped with broadband inverse gradient probeheads. Spectra were referenced to the residual solvent signals (chloroform-*d*, 7.24 ppm; dichloromethane-d_2 5.32 ppm, CHD_2OD, 3.30 ppm). Two-dimensional NMR spectra were recorded with 2048 data points in the t_2 domain and up to 2048 points in the t_1 domain, with a 1−1.5 s recovery delay. All 2D spectra were recorded with gradient selection, with the exception of ROESY. The ROESY spinlock time was 300 ms. ^{13}C NMR spectra were recorded with ^{1}H broadband decoupling and referenced to solvent signals ($^{13}CDCl_3$, 77.0 ppm; $^{13}CD_2Cl_2$, 53.7 ppm, $^{13}CD_3OD$, 49.0 ppm). High resolution mass spectra were recorded using APCI or MALDI ionization in the positive mode. Compounds 2,7-dibromo-9-tolyl-9*H*-carbazole, **9a**, and **12a** were prepared following literature procedures.[65,73] Tetrahydrofuran and *N*,*N*-dimethylformamide were dried using a commercial solvent purification system. Dichloromethane was distilled from calcium hydride when used as a reaction solvent. Recycling gel permeation chromatography was carried out by application of a Shimadzu HPLC chromatograph equipped with an LC-20AD pump, RID-10A and SPD-M20A detectors, and a Shodex GPC KF-2001 series column (column size 20.0 mm × 300 mm), using dichloromethane elution with a flow rate of 2 mL/min at ambient temperature. ^{1}H NMR spectra were recorded on high-field spectrometers (^{1}H frequency 500.13 or 600.13 MHz), equipped with broadband inverse gradient probeheads. Spectra were referenced to the residual solvent signals (chloroform-*d*, 7.24 ppm; dichloromethane-d_2 5.32 ppm, CHD_2OD, 3.30 ppm). Two-dimensional NMR spectra were recorded with 2048 data points in the t_2 domain and up to 2048 points in the t_1 domain, with a 1−1.5 s recovery delay. All 2D spectra were recorded with gradient selection, with the exception of ROESY. The ROESY spinlock time was 300 ms. ^{13}C NMR spectra were recorded with ^{1}H broadband decoupling and referenced to solvent signals ($^{13}CDCl_3$, 77.0 ppm; $^{13}CD_2Cl_2$, 54.0 ppm, $^{13}CD_3OD$, 49.0 ppm). High resolution mass spectra were recorded using APCI or MALDI ionization in the positive mode.

Computational Methods. Density functional theory (DFT) calculations were performed using Gaussian 09 (for full reference see Supporting Information). DFT geometry optimizations were carried out in unconstrained C_1 symmetry and were refined to meet standard convergence criteria. Optimized geometries (in the pdb format) are included in Supporting Information as a compressed zip file. Transition-state geometries were optimized using the standard Gaussian algorithm (TS keyword). The curvature of all stationary points was checked by a normal-mode frequency calculation. The number of imaginary frequencies was verified to be exactly 0 for local minima and exactly 1 for transition states. DFT calculations were performed using the hybrid functional B3LYP, combined with the 6-31G(d,p) basis set. Geometry optimizations, frequency and thermochemistry calculations, and single-point calculations of distorted reactant fragments were performed using the integral equation formalism of the polarizable continuum model (IEF PCM)[74,75] with standard dichloromethane parametrization. For consistency with earlier work[64,68] and to avoid possible errors associated with the solvation model,[69] $\Delta E^{\ddagger}$ values, calculated without the inclusion of ZPV corrections, are used throughout this study rather than $\Delta G^{\ddagger}$'s.

X-ray Crystallography. X-ray quality crystals were grown by slow diffusion of methanol into a toluene solution of compounds **5a**−**c** and **10a**. Diffraction measurements were performed on an Xcalibur Ruby diffractometer (ω scans) equipped with Onyx CCD detector and graphite-monochromatized Mo Kα radiation. For compound **5a**, diffraction measurements were performed on a diffractometer with Cu Kα radiation and CCD Sapphire detector. All the diffraction data were collected at 100−80 K. Data collection, unit cell refinement, and data reduction and analysis were carried out with the Xcalibur PX software, CrysAlis PRO. The structure were solved by direct methods with the SHELXS-97[76] program and refined using SHELXL-97 with anisotropic thermal parameters for non-H atoms. All H atoms were treated as riding and placed in geometrically optimized positions. X-ray quality crystals of **6a** and **7a** were grown respectively by slow evaporation of dichloromethane and chloroform. An analytical absorption correction was applied to the data with the use of a multifaceted crystal model based on the expression derived by R. C. Clark and J. S. Reid.[77]

*9-Tolyl-9H-carbazole-2,7-dicarbaldehyde (**S1b**).* In round-bottomed flask equipped with a stirring bar, compound 2,7-dibromo-9-tolyl-9*H*-carbazole (2.50 g, 6.02 mmol) was dissolved in dry tetrahydrofuran (100 mL) under a nitrogen atmosphere. After cooling to −90 °C with an acetone−liquid nitrogen bath, *n*-butyllithium (2.5 M solution in tetrahydrofuran, 18.06 mmol, 7.2 mL) was added to the solution, resulting in the formation of a white slurry. The mixture was stirred under nitrogen for 40 min, and *N*,*N*-dimethylformamide (3.7 mL, 48.17 mmol) was added. The reaction mixture was allowed to warm to room temperature and was stirred for additional 2 h. The mixture was diluted with water and extracted with dichloromethane.

DOI: 10.1021/acs.joc.5b00745
J. Org. Chem. 2015, 80, 6300−6312

Organic extracts were dried over anhydrous magnesium sulfate and filtered, and the solvent was removed on a rotary evaporator. The product, isolated in the form of yellow crystals, did not require further purification (1.867 g, 99%). ^{1}H NMR (500 MHz, chloroform-*d*, 300 K): δ 10.09 (s, 2H), 8.31 (d, 2H, ^4J = 8.0 Hz), 7.89 (s, 2H), 7.84 (dd, 2H, ^3J = 8.0 Hz, ^4J = 1.2 Hz), 7.45 (d, 2H, ^3J = 8.3 Hz), 7.41 (d, 2H, ^3J = 8.3 Hz), 2.51 (s, 3H). ^{13}C NMR (125 MHz, chloroform-*d*, 300 K) δ: 192.18, 142.52, 138.88, 135.45, 133.43, 131.02, 127.07, 127.06, 121.75, 121.62, 112.13, 21.28. HRMS (ESI-TOF, **S1b** observed as the bis(*N*-butylimino) derivative): *m*/*z*: $[M + H]^+$ calcd for $C_{29}H_{34}N_3^+$: 424.2747; found: 424.2752.

*3,6-Dibromo-9-tolyl-9H-carbazole-2,7-dicarbaldehyde (**1b**).* In a dry flask equipped with magnetic stirring, 9-tolyl-9*H*-carbazole-2,7-dicarbaldehyde **S1b** (1.365 g, 4.36 mmol) was dissolved in dichloromethane (300 mL). Bromine (446 μL, 8.71 mmol) was added slowly to the vigorously stirred solution. The mixture was stirred for additional 2 h. The crude product was purified by column chromatography (silica gel, 50% dichloromethane in hexanes). The second fraction was collected and concentrated on a rotary evaporator to yield yellow crystals (0.853 g, 89%). ^{1}H NMR (500 MHz, chloroform-*d*, 300 K): δ 10.47 (s, 2H), 8.37 (s, 2H), 7.92 (s, 2H), 7.43 (d, 2H, ^3J = 8.3 Hz) 7.32 (d, 2H, ^3J = 8.3 Hz), 2.49 (s, 3H) ^{13}C NMR (125 MHz, chloroform-*d*, 300 K) δ: 192.18, 141.76, 139.35, 132.66, 132.00, 131.16, 126.87, 126.78, 126.12, 117.09, 112.06, 21.28. HRMS (APCI-TOF): *m*/*z*: $[M + H]^+$ calcd for $C_{21}H_{14}Br_2NO_2$ 469.9386; found 469.9379.

*(3,6-Dibromo-9-tolyl-9H-carbazole-2,7-diyl)dimethanol (**S2b**).* In a 100 mL round-bottomed flask equipped with a magnetic stirring bar, compound **1b** (0.853 g, 1.81 mmol) and sodium borohydride (136.9 mg, 3.62 mmol) were suspended in tetrahydrofuran (60 mL). The mixture was heated at 50 °C overnight, after which time the color of the suspension changed from yellow to white. The mixture was poured into water (100 mL). Hydrochloric acid (1 M, 70 mL) was then added, and the mixture was extracted with dichloromethane. Combined extracts were dried with anhydrous sodium sulfate and filtered. Solvents were removed on a rotary evaporator, yielding a white solid (0.857 g, 99%). ^{1}H NMR (500 MHz, dimethyl sulfoxide-d_6, 300 K): δ 8.53 (s, 2H), 7.52 (d, 2H, ^3J = 8.3 Hz), 7.48 (s, 2H), 7.47 (d, 2H, ^3J = 8.3 Hz), 5.48 (t, 2H, ^3J = 5.5 Hz), 4.60 (dd, 4H, ^2J = 0.9 Hz, ^3J = 5.5 Hz) 2.47 (s, ~3H, OH + H_2O). ^{13}C NMR (125 MHz, dimethyl sulfoxide-d_6, 300 K) δ: 140.21, 139.01, 137.99, 133.60, 130.80, 126.86, 124.01, 121.68, 111.73, 108.70, 63.03, 20.76. HRMS (APCI-TOF): *m*/*z*: $[M - H_2O]^+$ calcd for $C_{21}H_{16}Br_2NO$: 455.9593; found 455.9578.

*3,6-Dibromo-9-tolyl-2,7-bis(chloromethyl)-9H-carbazole (**S3b**).* Compound **S2b** (0.177 g, 0.390 mmol) was suspended in freshly distilled dichloromethane (50 mL), to which a catalytic amount of *N*,*N*-dimethylformamide (10 μL) was added. With continuous stirring, thionyl chloride (61 μL, 0.852 mmol) was added to the reaction mixture. After 3 h of stirring, the solvent and excess thionyl chloride were removed on a rotary evaporator. The product (0.179 g, 99%) was used in the next step without further purification. ^{1}H NMR (500 MHz, chloroform-*d*, 300 K): δ 8.26 (s, 2H), 7.43 (d, 2H, ^3J = 8.7 Hz), 7.42 (s, 2H), 7.35 (d, 2H, ^3J = 8.1 Hz), 4.79 (s, 4H), 2.50 (s, 3H). ^{13}C NMR (125 MHz, chloroform-*d*, 300 K) δ: 140.98, 138.67, 134.67, 133.56, 130.94, 126.88, 124.88, 123.40, 114.87, 112.26, 47.17, 21.29. HRMS (APCI-TOF): *m*/*z*: $[M + H]^+$ calcd for $C_{21}H_{16}Br_2Cl_2N$: 509.9021; found 509.9023.

*((3,6-Dibromo-9-tolyl-9H-carbazole-2,7-diyl)bis(methylene))bis-(triphenylphosphonium) Chloride (**2b**).* In a 100 mL round-bottomed flask equipped with a reflux condenser and magnetic stirring, compound **S3b** (231 mg, 0.31 mmol) and triphenylphosphine (86.5 mg, 0.33 mmol) were dissolved in *N*,*N*-dimethylformamide (2 mL). The mixture was heated under a protective atmosphere and refluxed overnight. Subsequently, the mixture was cooled down and the precipitate was filtered, washed with hexanes, and dried under vacuum to give the product as colorless crystals (299 mg, 96%). ^{1}H NMR (600 MHz, chloroform-*d*, 300 K): δ 7.98 (s, 2H), 7.71 (b, 6H), 7.65 (b, 12H), 7.54 (b, 12H), 7.31 (b, 2H), 7.19 (b, 2H), 6.75 (b, 2H), 5.86 (b, 4H, J_{PH} = 13.3 Hz), 2.51 (s, 3H). ^{13}C NMR (151 MHz, dichloromethane-d_2, 300 K): δ 140.37 (d, J_{PC} = 2.2 Hz), 138.26 (d, J_{PC} = 2.4 Hz), 135.67, 134.91 (d, J_{PC} = 10.0 Hz), 132.84, 131.25, 130.69 (d, J_{PC} = 13.1 Hz), 125.80 (d, J_{PC} = 7.6 Hz), 125.42, 123.73, 118.04 (d, J_{PC} = 6.7 Hz), 117.78 (d, J_{PC} = 86.1 Hz), 114.82 (d, J_{PC} = 4.4 Hz), 31.01 (d, J_{PC} = 47.7 Hz), 21.62. HRMS (ESI-TOF): *m*/*z*: $[M]^{2+}$ calcd for $C_{57}H_{45}Br_2NP_2$: 481.5692; found 481.5689.

*7,7′-((1Z,1′Z)-(3,6-Dibromo-9-butyl-9H-carbazole-2,7-diyl)bis-(ethene-2,1-diyl))bis(3,6-dibromo-9-butyl-2-(chloromethyl)-9H-carbazole) (**10a**).* In a 50 mL round-bottomed flask equipped with magnetic stirring and a septum, compounds **9a** (254 mg, 343 μmol) and **1a** (50 mg, 114 μmol) were dissolved in dichloromethane (35 mL). Aqueous sodium hydroxide (50%, 1.0 mL) was added to the mixture with a syringe. During addition, the mixture was kept under an atmosphere of nitrogen and protected from light. After addition, the solution was stirred for additional 4 h. Subsequent workup was carried out in relative darkness. The reaction mixture was diluted with water and extracted with dichloromethane. Combined extracts were dried over anhydrous sodium sulfate and filtered. Solvents were removed on a rotary evaporator, yielding a yellow residue. The crude material was chromatographed (silica gel, 50% dichloromethane in hexanes) to give the product as a bright yellow solid (71 mg, 48%, 4:1 *ZZ*:*ZE* isomer ratio). ^{1}H NMR (500 MHz, chloroform-*d*, 300 K, *ZZ* isomer): δ 8.12 (s, 2H), 8.12 (s, 2H), 8.10 (s, 2H), 7.26 (s, 2H), 6.96 (b, 4H), 6.92 (s, 2H), 6.74 (s, 2H), 4.83 (s, 4H), 3.74m (t, 4H, ^3J = 7.1 Hz), 3.29 (t, 2H, ^3J = 7.1 Hz), 1.13 (m, 4H), 0.74 (m, 2H), 0.56 (m, 2H), 0.34 (t, 6H, ^3J = 7.3 Hz), 0.30 (m, 2H), 0.08 (t, 3H, ^3J = 7.3 Hz). HRMS (APCI-TOF): *m*/*z*: $[M]^+$ calcd for $C_{54}H_{47}Br_6Cl_2N_3$: 1282.8221; found 1282.8224.

*((7,7′-((1Z,1′Z)-(3,6-Dibromo-9-butyl-9H-carbazole-2,7-diyl)bis-(ethene-2,1-diyl))bis(3,6-dibromo-9-butyl-9H-carbazole-7,2-diyl))-bis(methylene))bis(triphenylphosphonium) Dichloride (**11a**).* In a 100 mL Ace pressure tube equipped with magnetic stirring, compounds **10a** (50 mg, 38.8 μmol) and triphenylphosphine (61.1 mg, 232.9 μmol) were dissolved in toluene (2 mL). The mixture was protected from light and heated at 150 °C overnight. After this time, the solvent was removed on a rotary evaporator, yielding a yellow residue. The crude material was crystallized from dichloromethane−*n*-hexane and to give the product as a light brown solid (isomeric mixture, 63.1 mg, 90%). ^{1}H NMR (500 MHz, MeOH-d_4 300 K, *ZZ* isomer, CH_2P protons exchanged by deuterium): δ 8.34 (s, 6H), 8.21 (s, 2H), 7.89 (td, 6H, J_{HH} = 7.5 Hz), 7.67 (td, 12H, J_{HH} = 7.9 Hz, J_{PH} = 3.6 Hz), 7.54 (dd, 12H, J_{HH} = 8.5 Hz, J_{PH} = 12.8 Hz), 7.1 (d, 4H, J_{HH} = 2.9 Hz), 7.01 (b, 4H), 6.94 (s, 2H), 6.85 (s, 2H), 4.57 (s, 4H), 3.59 (t, 4H, ^3J = 6.8 Hz), 3.41 (t, 2H, ^3J = 6.8 Hz), 0.68 (m, 6H), 0.39 (m, 6H), 0.11 (t, 4H, ^3J = 7.5 Hz), 0.01 (t, 2H, ^3J = 7.5 Hz). HRMS (ESI-TOF): *m*/*z*: $[M]^{2+}$ calcd for $C_{90}H_{77}Br_6N_3P_2$: 867.5341; found 867.5357.

*(Z)-3,6-Dibromo-9-butyl-7-(2-(3,6-dibromo-9-butyl-7-(chloromethyl)-9H-carbazol-2-yl)vinyl)-9H-carbazole-2-carbaldehyde (**13a**).* In a 250 mL round-bottomed flask equipped with magnetic stirring and a septum, compounds **9a** (134 mg, 182.0 μmol) and **1a** (70.9 mg, 162.1 μmol) were dissolved in dichloromethane (90 mL). Aqueous sodium hydroxide (50%, 0.6 mL) was added to the mixture with a syringe. During addition, the mixture was kept under an atmosphere of nitrogen and protected from light. After addition, the solution was stirred for additional 12 h. Subsequent workup was carried out in relative darkness. The reaction mixture was diluted with water and extracted with dichloromethane. Combined extracts were dried over anhydrous sodium sulfate and filtered. Solvents were removed on a rotary evaporator, yielding a yellow residue. The crude product was purified by column chromatography (silica gel, 50% dichloromethane in hexanes). The second fraction was collected and concentrated on a rotary evaporator to yield yellow crystals (100.5 mg, 71.8%). ^{1}H NMR (600 MHz, chloroform-*d*, 300 K): δ 10.42 (s, 1H), 8.26 (s, 1H), 8.21 (s,1H), 8.16 (s, 1H), 8.13 (s, 1H), 7.79 (s, 1H), 7.29 (s,1H), 7.07 (d, 2H, ^3J = 11.7 Hz), 7.03 (d, 2H, ^3J = 11.7 Hz), 6.98 (s, 1H), 6.95 (s, 1H), 3.83 (t, 2H, ^3J = 7.2 Hz), 3.81 (t, 2H, ^3J = 7.3 Hz), 1.16 (m, 4H), 0.80 (m, 4H), 0.40 (t, 3H, ^3J = 5.3 Hz), 0.38 (t, 3H, ^3J = 5.3 Hz). ^{13}C NMR (151 MHz, chloroform-*d*, 300 K) δ: 192.33, 141.10, 140.04, 139.88, 139.59, 136.88, 135.01, 134.03, 132.78, 131.94,

DOI: 10.1021/acs.joc.5b00745
J. Org. Chem. 2015, 80, 6300−6312

130.22, 127.38, 124.89, 124.84, 124.57, 124.12, 123.08, 122.25, 121.54, 116.21, 114.73, 114.08, 113.67, 111.83, 111.42, 110.82, 110.07, 47.24, 43.01, 42.82, 30.50, 30.46, 20.03 (2C), 13.23, 13.19. HRMS (APCI-TOF): m/z: $[M-Cl]^+$ calcd for $C_{36}H_{31}Br_4N_2O$: 822.9164; found 822.9191.

*(Z)-3,6-Dibromo-7-(2-(3,6-dibromo-9-butyl-7-(chloromethyl)-9H-carbazol-2-yl)vinyl)-9-(p-tolyl)-9H-carbazole-2-carbaldehyde (**13c**).* In a 250 mL round-bottomed flask equipped with magnetic stirring and a septum, compounds **9a** (300 mg, 495 μmol) and **1b** (286 mg, 608 μmol) were dissolved in dichloromethane (270 mL). Aqueous sodium hydroxide (50%, 1.5 mL) was added to the mixture with a syringe. During addition, the mixture was kept under an atmosphere of nitrogen and protected from light. After addition, the solution was stirred for an additional 48 h. Subsequent workup was carried out in relative darkness. The reaction mixture was diluted with water and extracted with dichloromethane. Combined extracts were dried over anhydrous sodium sulfate and filtered. Solvents were removed on a rotary evaporator, yielding a yellow residue. The crude product was purified by column chromatography (silica gel, 50% dichloromethane in hexanes). The second fraction was collected and concentrated on a rotary evaporator to yield yellow crystals (287.7 mg, 79%). ^{1}H NMR (600 MHz, chloroform-*d*, 300 K): δ 10.37 (s, 1H), 8.29 (s, 1H), 8.21 (s,1H), 8.19 (s, 1H), 8.15 (s, 1H), 7.73 (s, 1H), 7.35 (s, 1H), 7.00 (d, 1H, ^3J = 11.8 Hz), 6.98 (d, 1H, ^3J = 11.8 Hz), 6.97 (s, 1H), 6.92 (s, 1H) 6.87 (d, 2H, ^3J = 8.1 Hz), 6.59 (d, 2H, ^3J = 8.1 Hz), 4.84 (s, 2H), 3.86 (t, 2H, ^3J = 7.2 Hz), 2.30 (s, 3H), 1.23 (m, 2H), 0.85 (m, 2H), 0.43 (t, 3H, ^3J = 7.3 Hz). ^{13}C NMR (151 MHz, chloroform-*d*, 300 K): 192.14, 141.37, 140.16, 140.06, 139.92, 138.10, 136.56, 135.09, 134.14, 132.80, 132.64, 131.61, 130.44, 130.43, 127.72, 125.69, 125.67, 124.86, 124.53, 124.16, 123.17, 122.20, 121.79, 116.93, 115.67, 113.91, 113.76, 112.97, 111.44, 111.11, 110.91, 47.27, 42.89, 30.54, 21.16, 20.07, 13.29. HRMS (APCI-TOF): m/z: $[M]^+$ calcd for $C_{39}H_{29}Br_4N_2O$: 856.9008; found 856.8966

*(Z)-((3,6-Dibromo-9-butyl-7-(2-(3,6-dibromo-7-formyl-9-(p-tolyl)-9H-carbazol-2-yl)vinyl)-9H-carbazol-2-yl)methyl)-triphenylphosphonium Chloride (**14c**).* In a pressure tube equipped with a magnetic stirring, compound **13c** (287.7 mg, 321 μmol) and triphenylphosphine (282.3 mg, 385 μmol) were dissolved in benzene (5 mL). The mixture was heated under a protective atmosphere to 70 °C for 3 days. After this time, the solvent was removed on a rotary evaporator, yielding a yellow residue. The crude material was crystallized from dichloromethane−hexane. The precipitate was filtered, washed with hexanes, and dried under vacuum to give the product as bright brown crystals (314.27 mg, 84%). ^{1}H NMR (600 MHz, chloroform-*d*, 300 K): δ 10.38 (s, 1H), 8.28 (s, 1H), 8.21 (s, 1H), 8.08 (b, 1H), 7.95 (b, 1H). 7.77 (s, 1H), 7.71 (b, 3H), 7.66 (b, 6H), 7.53 (b, 6H), 6.96 (s, 1H), 6.94 (d, ^3J = 7.6 Hz), 6.91 (s, 1H), 6.60 (d, 2H, ^3J = 7.6 Hz), 5.80 (b, 2H), 3.75 (b, 2H), 2.33 (s, 3H), 0.88 (b, 2H), 0.51 (b, 2H), 0.15 (b, 3H); ^{13}C NMR (151 MHz, chloroform-*d*, 300 K) δ: 192.20, 141.30, 140.17 (d, J_{PC} = 3.5 Hz), 140.02, 139.87, 137.91, 136.75, 135.23, 134.93, 134.45 (d, J_{PC} = 9.8 Hz), 132.86, 132.69, 131.70, 130.52, 130.39, 130.09 (d, J_{PC} = 12.7 Hz), 128.30, 127.78, 125.75, 124.92 (d, J_{PC} = 8.9 Hz), 124.50 (d, J_{PC} = 8.8 Hz), 124.44, 124.10, 123.80 (d, J_{PC} = 2.7 Hz), 122.89, 121.81, 121.78, 117.71 (d, J_{PC} = 86.0 Hz), 117.04, 116.35 (d, J_{PC} = 5.8 Hz), 115.52, 114.69, 113.89, 112.91, 111.31, 42.95, 31.24 (d, J_{PC} = 49.0 Hz), 30.32, 21.26, 19.86, 13.30. HRMS (ESI-TOF): m/z: $[M]^+$ calcd for $C_{57}H_{44}Br_4N_2OP$: 1118.9919; found 1118.9921

*(Z)-((3,6-Dibromo-9-butyl-7-(2-(3,6-dibromo-9-butyl-7-formyl-9H-carbazol-2-yl)vinyl)-9H-carbazol-2-yl)methyl)-triphenylphosphonium Chloride (**14a**).* In a 25 mL round-bottomed flask equipped with a reflux condenser and magnetic stirring, compound **13a** (83.7 mg, 97.0 μmol) and triphenylphosphine (50.89 mg, 194.0 μmol) were dissolved in benzene (7 mL). The mixture was heated under a protective atmosphere and refluxed for 78 h. After that time, the solvent was removed on a rotary evaporator, yielding a yellow residue. The crude material was crystallized from dichloromethane−hexanes. The precipitate was filtered, washed with hexanes, and dried under vacuum to give the product as light brown crystals (65.9 mg, 98.0%). ^{1}H NMR (600 MHz, chloroform-*d*, K): δ 10.43 (s, 1H), 8.25 (s, 1H), 8.12 (s, 1H), 7.87 (d, 1H, J_{PH} = 0.6 Hz), 7.80 (s, 1H), 7.73 (d, 1H J_{PH} = 2.8 Hz), 7.71 (t, 3H, J_{HH} = 7.3 Hz), 7.64 (dd, 6H, J_{HH} = 7.4 Hz, J_{PH} = 12.5 Hz), 7.54 (td, 6H, J_{HH} = 7.9 Hz, J_{PH} = 3.5 Hz), 7.03 (d, 1H, ^3J = 11.4 Hz), 6.99 (d, 1H, ^3J = 11.4 Hz), 6.98 (s, 1H), 6.86 (s, 1H), 5.79 (d, 2H, J_{PH} = 14.0 Hz), 3.88 (t, 2H, ^3J = 7.2 Hz), 3.68 (t, 2H, ^3J = 6.9 Hz), 1.2 (m, 2H), 0.83 (m, 2H), 0.76 (m, 2H), 0.48 (m, 2H), 0.38 (t, 3H, ^3J = 7.2 Hz), 0.14 (t, 3H, ^3J = 7.2 Hz). ^{13}C NMR (151 MHz, chloroform-*d*, 300 K): δ 192.43, 141.16, 140.16 (d, J_{PC} = 3.2 Hz), 139.86, 139.51, 137.02, 135.14, 134.94, 134.93 (d, J_{PC} = 2.7 Hz), 134.44 (d, J_{PC} = 9.7 Hz), 134.41, 132.64, 132.06, 130.20, 130.07 (d, J_{PC} = 12.5 Hz), 127.42, 124.92, 124.26 (d, J_{PC} = 9.1 Hz), 124.04, 123.86 (d, J_{PC} = 2.7 Hz), 122.88 (d, J_{PC} = 3.2 Hz), 121.87, 121.54, 117.72 (d, J_{PC} = 85.4 Hz), 116.34 (d, J_{PC} = 4.1 Hz), 114.59(d, J_{PC} = 4.5 Hz).113.97, 111.72, 111.56, 110.02, 42.98, 42.91, 31.18 (d, J_{PC} = 48,2 Hz), 30.53, 30.31, 20.02, 19.84, 13.35, 13.29. HRMS (MALDI-TOF): m/z: $[M - 2H]^+$ calcd for $C_{54}H_{43}Br_4ClN_2OP$: 1116.9542; found 1116.9530.

C1C + P1P Synthesis of 5a and 6a. In a 100 mL round-bottomed flask equipped with magnetic stirring and a septum, compounds **2a** (114.7 mg, 114 μmol) and **1a** (50 mg, 114 μmol) were dissolved in dichloromethane (70 mL). Aqueous sodium hydroxide (50%, 0.4 mL) was added to the mixture with a syringe. During addition, the mixture was kept under an atmosphere of nitrogen and protected from light. After addition, the solution was stirred for additional 5 h. The reaction mixture was diluted with water and extracted with dichloromethane. Combined extracts were dried over anhydrous sodium sulfate and filtered. Solvents were removed on a rotary evaporator, yielding a yellow residue. The crude product was purified by column chromatography (silica gel, dichloromethane). The first fraction was collected and concentrated on a rotary evaporator. The material was crystallized from dichloromethane/hexane to yield **5a** as a yellow solid (24 mg, 27%). Subsequent crude fractions were combined and stripped of solvent on a rotary evaporator. The residue was subjected to recirculating gel permeation chromatography to separate **6a** (3 mg 1.1%) from higher oligomers and residual **5a**.

*(3,3′,3″,3‴,6,6′,6″,6‴-Octabromo-9,9′,9″,9‴-tetra-n-butyl)[2$_4$]-(2,7)carbazolophanetetraene (**5a**).* ^{1}H NMR (500 MHz, chloroform-*d*, 300 K): δ 8.17 (s, 8H), 7.01 (s, 8H), 6.96 (s, 8H), 3.37 (t, 8H, ^3J = 7.2 Hz), 1.02 (m, 8H), 0.71 (m, 8H), 0.30 (t, 12H, ^3J = 7.26 Hz), ^{13}C NMR (125 MHz, chloroform-*d*, 300 K) δ: 140.03, 134.48, 130.68, 124.14, 122.32, 114.43, 109.74, 42.72, 30.36, 19.99, 13.23, HRMS (APCI-TOF): m/z: $[M + H]^+$ calcd for $C_{72}H_{61}Br_8N_4$: 1612.8358; found 1612.8397.

*(3^6,6^6-Dodecabromo-9^6-hexabutyl)-(Z^{5}E)-[2$_6$](2,7)-carbazolophanehexaene (**6a**).* ^{1}H NMR (600 MHz, chloroform-*d*, 300 K): δ 8.16 (s, 2H), 8.15 (s, 2H), 8.08 (s, 2H), 8.04 (s, 2H), 7.94 (s, 2H), 7.89 (s, 2H), 7.66 (s, 2H), 7.01 (s, 2H), 6.91 (s, 2H), 6.91 (s, 2H), 6.89 (s, 2H), 6.88 (s, 2H), 6.86 (s, 2H), 6.70 (s, 2H), 6.63 (s, 2H), 6.57 (s, 2H), 3.93 (b, 2H), 3.88 (b, 2H), 3.40 (b, 4H), 3.29 (b, 2H), 3.23 (b, 2H), 1.30 (b, 2H), 1.29 (b, 2H), 0.63 (m, 4H), 0.52 (b, 2H), 0.49 (m, 2H), 0.41 (b, 2H), 0.41 (b, 4H), 0.05 (t, 6H, ^3J = 7.3 Hz), 0.03 (m, 2H), −0.06 (b, 2H), −0.08 (m, 2H), −0.22 (b, 6H), −0.52 (t, 6H, ^3J = 7.3 Hz). ^{13}C NMR (151 MHz, chloroform-*d*, 250 K, HSQC partial data): δ 132.7, 132.4, 131.5, 131.2, 130.8, 131.0, 124.0, 123.7, 123.5, 123.3, 123.2, 123.1, 111.0, 110.9, 110.9, 110.7, 110.1, 106.6, 68.0, 42.6, 42.8, 42.7, 42.5, 30.6, 29.9, 29.5, 28.8, 20.2, 19.8, 13.1, 12.9, 12.3. HRMS (APCI-TOF): m/z: $[M - Br]^+$ calcd for $C_{108}H_{92}Br_{11}N_6$: 2342.8375; found 2342.8329.

***C1C + P1P** Synthesis of (3,3′,3″,3‴,6,6′,6″,6‴-Octabromo-9,9′,9″,9‴-tetratolyl)[2$_4$](2,7)carbazolophanetetraene (**5b**).* In a 50 mL round-bottomed flask equipped with magnetic stirring and a septum, compounds **1b** (45.5 mg, 96.5 μmol) and **2b** (100 mg, 96.5 μmol) were dissolved in dichloromethane (64 mL). Aqueous sodium hydroxide (50%, 0.2 mL) was added to the mixture with a syringe. During addition, the mixture was kept under an atmosphere of nitrogen and protected from light. After addition, the solution was stirred for additional 3 h. Subsequent workup was carried out in relative darkness. The reaction mixture was diluted with water and extracted with dichloromethane. Combined extracts were dried over anhydrous sodium sulfate and filtered. Solvents were removed on a

DOI: 10.1021/acs.joc.5b00745
J. Org. Chem. 2015, 80, 6300−6312

rotary evaporator, yielding a yellow residue. The crude product was purified by column chromatography (silica gel, dichloromethane). The first fraction was collected and concentrated on a rotary evaporator to yield yellow crystals. Product was crystallized from dichloromethane−hexanes (2.5 mg, 2.9%). ^{1}H NMR (600 MHz, chloroform-*d*, 330 K): δ 8.08 (s, 8H), 7.12 (s, 8H), 6.94 (s, 8H), 6.55 (b), 6.32 (b), 1.69 (s, 12H). ^{13}C NMR (151 MHz, chloroform-*d*, 330 K, HSQC, partial data): δ 151.9, 145.4, 143.8, 142.2,142.1, 141.8, 138.4, 136.8, 136.1, 122.0, 32.18. HRMS (APCI-TOF): *m*/*z*: [M + H]$^+$ calcd for $C_{84}H_{53}Br_8N_4$: 1748.7732; found 1748.7741.

C1C + P1P Synthesis of (3,3′,3″,3‴,6,6′,6″,6‴-Octabromo-9,9″-di-*n*-butyl-9′,9‴-tolyl)[2$_4$](2,7)carbazolophanetetraene 5c. In a 100 mL round-bottomed flask equipped with magnetic stirring and a septum, compounds **2a** (106.4 mg, 106.12 μmol) and **1b** (50 mg, 106.12 μmol) were dissolved in dichloromethane (70 mL) Aqueous sodium hydroxide (50%, 180 μL) was added to the mixture with a syringe. During addition, the mixture was kept under an atmosphere of nitrogen and protected from light. After addition, the solution was stirred for additional 5 h. The reaction mixture was diluted with water and extracted with dichloromethane. Combined extracts were dried over anhydrous sodium sulfate and filtered. Solvents were removed on a rotary evaporator, yielding a yellow residue. The crude product was purified by column chromatography (silica gel, dichloromethane) to remove the phosphine oxide. The first fraction was collected and concentrated on a rotary evaporator. The product was subjected to recirculating gel permeation chromatography to separate **5c** from higher oligomers and then crystallized from dichloromethane−hexane (24 mg, 26.7%). ^{1}H NMR (500 MHz, chloroform-*d*, 300 K): δ 8.24 (s, 4H), 8.067 (s, 4H), 7.11 (s, 4H), 7.03 (s, 4H), 6.97 (d, 8H, ^3J = 12.4 Hz), 6.92 (d, 8H, ^3J = 12.4 Hz), 3.43 (t, 4H, ^3J = 7.3 Hz), 1.75 (s, 6H), 1.03 (m, 4H), 0.66 (m, 4H), 0.27 (t, 6H, ^3J = 7.3 Hz). ^{13}C NMR (151 MHz, dichloromethane-d_2, 330 K): δ 130.9, 130.8, 125.4, 125.3, 124.8, 124.7, 111.25, 109.84, 42.9, 31.0, 21.2, 20.4, 20.3. HRMS (APCI-TOF): *m*/*z*: [M + H]$^+$ calcd for $C_{78}H_{57}Br_8N_4$: 1680.8045; found 1680.8083.

P3P + C1C Synthesis of **5a**. In a 25 mL round-bottomed flask equipped with magnetic stirring and a septum, compounds **11a** (20.0 mg, 11.0 μmol) and **1a** (4.82 mg, 11.0 μmol) were dissolved in dichloromethane (7.3 mL). Aqueous sodium hydroxide (50%, 1.0 mL) was added to the mixture with a syringe. After addition, the color of the solution changes from yellow to orange. The solution was stirred for additional 12 h. The reaction mixture was diluted with water and extracted with dichloromethane. Combined extracts were dried over anhydrous sodium sulfate and filtered. Solvents were removed on a rotary evaporator, yielding a yellow residue. The crude product was purified by column chromatography (silica gel, 50% dichloromethane in hexanes). The first fraction was collected and concentrated on a rotary evaporator to yield yellow crystals (4.9 mg, 28.0%)

In a 25 mL round-bottomed flask equipped with magnetic stirring and a septum, compounds **11a** (20.0 mg, 11.0 μmol) and **1a** (4.82 mg, 11.0 μmol) were dissolved in *N*,*N*-dimethylformamide (7 mL), and solid potassium *tert*-butoxide (2.7 mg, 24.2 μmol) was added under argon in one portion. After addition, the color of the solution changes from yellow to red. The solution was stirred for additional 1 h. The reaction mixture was diluted with water and extracted with dichloromethane. Combined extracts were dried over anhydrous sodium sulfate and filtered. Solvents were removed on a rotary evaporator, yielding a yellow residue. The crude product was purified by column chromatography (silica gel, 50% dichloromethane in hexanes). The first fraction was collected and concentrated on a rotary evaporator to yield yellow crystals (4.85 mg, 27.0%).

P3P + C1C Synthesis of 5d. In a 25 mL round-bottomed flask equipped with magnetic stirring and a septum, compounds **11a** (20 mg, 11.0 μmol) and **1b** (5.2 mg, 11.0 μmol) were dissolved in dichloromethane (7.3 mL). Aqueous sodium hydroxide (50%, 1.0 mL) was added to the mixture with a syringe. After addition, the color of the solution changes from yellow to orange. The solution was stirred for additional 12 h. The reaction mixture was diluted with water and extracted with dichloromethane. Combined extracts were dried over anhydrous sodium sulfate and filtered. Solvents were removed on a rotary evaporator, yielding a yellow residue. The crude product was purified by column chromatography (silica gel, 50% dichloromethane in hexanes). The first fraction was collected and concentrated on a rotary evaporator. Product was subjected to recirculating gel permeation chromatography and then was crystallized from dichloromethane−hexanes (3 mg, 16.4%); ^{1}H NMR (600 MHz, dichloromethane-*d*, 330 K): δ 0.26 (t, 3H, ^3J = 7.3 Hz), 0.32 (t, 6H, ^3J = 7.3 Hz), 2.01 (s, 3H), 3.43 (t, 6H, ^3J = 7.3 Hz), 6.42 (d, 2H, ^3J = 7.6 Hz), 6.49 (d, 2H, ^3J = 7.6 Hz), 6.90 (d, 4H, ^3J = 12.2 Hz), 6.95 (d, 4H, ^3J = 12.2 Hz), 7.00 (s, 2H), 7.01 (s, 2H), 7.05 (s, 2H), 7.07 (s, 2H), 8.09 (s, 2H), 8.19 (s, 2H), 8.21 (s, 2H), 8.23 (s, 2H). ^{13}C NMR (151 MHz, chloroform-*d*, 330 K, HSQC, partial data): δ 148.4, 131.1, 124.1, 124.0, 123.9, 123.9, 110.9, 109.7, 109.1, 109.6, 42.7, 30.5, 20.6, 19.9, 13.1, 12.9.

C2P Synthesis of 5a and 6a. In a 100 mL round-bottomed flask equipped with magnetic stirring and a septum, compound **14a** (100 mg, 88.9 μmol) was dissolved in dichloromethane (70 mL). Aqueous sodium hydroxide (50%, 0.15 mL) was added to the mixture with a syringe. During addition, the mixture was kept under an atmosphere of nitrogen and protected from light. After addition, the solution was stirred for additional 12 h. The reaction mixture was diluted with water and extracted with dichloromethane. Combined extracts were dried over anhydrous sodium sulfate and filtered. Solvents were removed on a rotary evaporator, yielding a yellow residue. The crude product was purified by column chromatography (silica gel, 50% dichloromethane in hexanes). The first fraction was collected and concentrated on a rotary evaporator. The material was crystallized from dichloromethane/hexane to yield **5a** as a yellow solid (45 mg, 42%). Subsequent crude fractions were combined and stripped of solvent on a rotary evaporator. The residue was subjected to recirculating gel permeation chromatography to separate **6a** from higher oligomers and residual **5a**.

C2P Synthesis of 5c. In a 100 mL round-bottomed flask equipped with magnetic stirring and a septum, compound **14c** (71 mg, 61.3 μmol) was dissolved in dichloromethane (48 mL). Aqueous sodium hydroxide (50%, 0.1 mL) was added to the mixture with a syringe. During addition, the mixture was kept under an atmosphere of nitrogen and protected from light. After addition, the solution was stirred for additional 12 h. The reaction mixture was diluted with water and extracted with dichloromethane. Combined extracts were dried over anhydrous sodium sulfate and filtered. Solvents were removed on a rotary evaporator, yielding a yellow residue. The crude product was purified by column chromatography (silica gel, dichloromethane−hexanes = 1:2). The first fraction was collected and concentrated on a rotary evaporator to yield yellow crystals (21 mg, 40%).

C3C + P3P Synthesis of 6a. In a 25 mL round-bottomed flask equipped with magnetic stirring and septum, compounds **11a** (15 mg, 8.3 μmol) and **12a** (13.3 mg, 8.3 μmol) were dissolved in dichloromethane (2.8 mL). Aqueous sodium hydroxide (50%, 0.3 mL) was added to the mixture with a syringe. During addition, the mixture was kept under an atmosphere of nitrogen and protected from light. After addition, the solution was stirred for an additional 12 h. The reaction mixture was diluted with water and extracted with dichloromethane. Combined extracts were dried over anhydrous sodium sulfate and filtered. Solvents were removed on a rotary evaporator, yielding a yellow residue. The crude product was purified by column chromatography(silica gel, dichloromethane−hexanes = 1:1), and first fraction was collected and concentrated on a rotary evaporator. The product was crystallized from dichloromethane−hexanes (ca. 4% by NMR).

*3,3′,6,6′-Tetrabromo-9,9′-dibutyl)[2.2](2,7)carbazolophanediene (**7a**).* In a 100 mL three-necked round-bottomed flask fitted with a reflux condenser and a septum were placed zinc powder (748 mg, 11.44 mmol) and copper(I) chloride (69 mg, 0.36 mmol). The apparatus was filled with argon, and oxygen-free tetrahydrofuran (10 mL) was introduced through a syringe. Titanium tetrachloride (0.6 mL, 5.72 mmol) was added dropwise over 2 min using a syringe. The mixture was then heated under reflux for 3 h. Subsequently, a solution of compound **1a** (100 mg, 0.22 mmol) in oxygen-free tetrahydrofuran (20 mL) was slowly added to the boiling mixture using a syringe. After

DOI: 10.1021/acs.joc.5b00745
J. Org. Chem. 2015, 80, 6300−6312

completion of the addition (2 h), the septum was replaced with a glass stopper and the reaction mixture was kept under reflux for 12 h. After that time, the mixture was cooled to room temperature. Aqueous ammonia (6%, 100 mL) was added. The mixture was extracted with dichloromethane. The organic layer was washed with brine, dried over Na_2SO_4, and evaporated to give an yellow-orange oil. The crude product was purified by column chromatography (silica gel, dichloromethane–hexanes = 1:1) and then by preparative TLC. Compounds **7a** and **3a** eluted respectively as the first and second fraction. After filtration, solvents were removed under reduced pressure to give **3a** (6.9 mg, 7.3%) and **7a** (17.0 mg, 18.3%) as yellow solids. Compound **3a** was characterized previously.[65]

*Compound **7a**.* ^{1}H NMR (500 MHz, chloroform-*d*, 300 K): δ 7.46 (s, 4H), 7.20 (s, 4H), 6.86 (s, 4H), 4.21 (t, 4H, ^3J = 6.7 Hz), 1.57 (m, 4H), 1.08 (m, 4H), 0.79 (t, 6H, ^3J = 7.3 Hz); ^{13}C NMR (125 MHz, chloroform-*d*, 300 K) δ 138.72, 136.10, 133.29, 122.71, 121.97, 114.65, 113.19, 43.27, 32.01, 20.08, 13.59. HRMS (MALDI-TOF): *m*/*z*: $[M]^+$ calcd for $C_{36}H_{30}Br_4N_2$: 805.9137; found 805.9114.

*3,3′,6,6′-Tetrabromo-9,9′-dibutyl)[2.2](2,7)carbazolophane (**8a**).* In a pressure tube equipped with magnetic stirring, compound **7a** (8.5 mg, 15 μmol) and *p*-toluenesulfonyl hydrazide (186.2 mg, 2.1 mmol) were dissolved in tetrahydrofuran (1.2 mL). Subsequently, a solution of sodium acetate (82.0 mg, 2.1 mmol) in water (1.3 mL) was added using a syringe. The pressure tube was quickly closed, and the mixture was heated to 92 °C for 2 h. After that time, the mixture changed color from yellow to almost colorless. The reaction mixture was diluted with water and extracted with dichloromethane. Combined extracts were dried over anhydrous sodium sulfate and filtered. Solvents were removed on a rotary evaporator, yielding pale yellow crystals. The crude product was purified by column chromatography (silica gel, 50% dichloromethane in hexane). The first fraction was collected and concentrated on a rotary evaporator. The material was crystallized from dichloromethane/methanol to yield **8a** as pale yellow crystals (8.2 mg, 96%). ^{1}H NMR (500 MHz, chloroform-*d*, 300 K): δ 7.42 (s, 4H), 6.7 (s, 4H), 4.14 (t, 4H, ^3J = 6.7 Hz), 3.86 (m, 4H), 3.16 (m, 4H), 1.55 (m, 4H), 1.07 (m, 4H), 0.78 (t, 6H, ^3J = 7.3 Hz). ^{13}C NMR (500 MHz, chloroform-*d*, 300 K): δ 138.97, 134.79, 123.13, 121.14, 115.36, 114.33, 42.92, 33.79, 31.78, 20.13, 13.63. HRMS (APCI-TOF): *m*/*z*: $[M + 2H]^+$ calcd for $C_{36}H_{36}Br_4N_2$: 811.9607; found 811.9621.

Hydrogenation of Crude Oligomer Mixtures. A 25 mL two-necked round-bottomed flask was charged with a mixture containing **5a**, **6a**, and other oligomers, derived from a **C2P** synthesis of **5a** and (**6a** 15 mg) and separated from triphenylphosphine oxide using column chromatography. The mixture was dissolved in dichloromethane (15 mL) and methanol (5 mL). Palladium on carbon (10 wt % loading, matrix-activated carbon support, 3 mg, 0.9 μmol) was added, and hydrogen gas was bubbled through the solution for 5 h. After that time, the reaction mixture was filtered and the solvents were removed on a rotary evaporator, yielding a white residue. The crude product was purified by column chromatography (silica gel, 50% dichloromethane in hexane). Three fractions were collected and concentrated on a rotary evaporator. The fractions contained cyclotetramer **16a** (5.5 mg, 60%), cyclohexamer **17a** (2 mg, 15%), and cyclooctamer **18a** (traces).

*9,9′,9″,9‴-Tetrabutyl[2$_4$](2,7)carbazolophane (**16a**).* R_f 0.57 (silica gel, 50% dichloromethane in hexane). ^{1}H NMR (500 MHz, chloroform-*d*, 300 K): δ 7.82 (d, 8H, ^3J = 7.6 Hz), 6.87 (dd, 8H, ^3J = 7.8 Hz, ^4J = 0.9 Hz), 6.64 (s, 8H), 3.60 (t, 8H, ^3J = 7.4 Hz), 3.15 (s, 16H), 1.25 (m, 8H), 0.95 (m, 8H), 0.62 (t, 12H, ^3J = 7.4 Hz) ^{13}C NMR (151 MHz, chloroform-*d*, 300 K): δ 140.51, 138.76, 120.86, 119.95, 119.48, 109.02, 42.04, 38.87, 30.50, 20.08, 13.53. HRMS (MALDI-TOF): *m*/*z*: $[M - H]^+$ calcd for $C_{72}H_{75}N_4$: 995.5986; found 995.5995.

*9^6-Hexabutyl[2$_6$](2,7)carbazolophane (**17a**).* R_f 0.45 (silica gel, 50% dichloromethan in hexane). ^{1}H NMR (600 MHz, chloroform-*d*, 300 K): δ 7.88 (d, 12H, ^3J = 7.8 Hz), 7.01 (dd, 12H, ^3J = 7.9 Hz, ^4J = 1.0 Hz), 6.82 (s, 12H), 3.84 (t, 12H, ^3J = 7.3 Hz), 3.16 (s, 24H), 1.31 (m, 12H), 0.95 (m, 12H), 0.55 (t, 18H, ^3J = 7.3 Hz). ^{13}C NMR (151 MHz, chloroform-*d*, 300 K): δ 140.62, 138.94, 120.90, 119.67, 119.59, 108.71, 42.32, 39.11, 30.57, 20.13, 13.40. HRMS (MALDI-TOF): *m*/*z*: $[M - H]^+$ calcd for $C_{108}H_{113}N_6$: 1493.9052; found 1493.9052.

*9^8-Octabutyl[2$_8$](2,7)carbazolophane (**18a**).* R_f 0.3 (silica gel, 50% dichloromethan in hexane). ^{1}H NMR (500 MHz, chloroform-*d*, 300 K): δ 7.89 (d, 16H, ^3J = 7.9 Hz), 7.02 (dd, 16H, ^3J = 8.0 Hz, ^4J = 1.2 Hz), 6.92 (s, 16H), 3.93 (t, 16H, ^3J = 7.1 Hz), 3.16 (s, 32H), 1.43 (m, 16H), 1.06 (m, 16H), 0.65 (t, 24H, ^3J = 7.2 Hz). HRMS (MALDI-TOF): *m*/*z*: $[M - H]^+$ $C_{144}H_{151}N_8$: 1992.2056; found 1992.2039.

■ ASSOCIATED CONTENT

Ⓢ Supporting Information

NMR and mass spectra. X-ray data (CIF). Computational data tables, figures, and Cartesian coordinates (PDB). The Supporting Information is available free of charge on the ACS Publications website at DOI: 10.1021/acs.joc.5b00745.

■ AUTHOR INFORMATION

Corresponding Author

*E-mail: marcin.stepien@chem.uni.wroc.pl.

Notes

The authors declare no competing financial interest

■ ACKNOWLEDGMENTS

The project was funded by the National Science Center of Poland (decisions DEC-2012/07/E/ST5/00781 and DEC-2012/07/N/ST5/00161). D.M. thanks the Foundation for Polish Science (START Programme) and European Union ("Human Capital" scholarship) for support. Quantum chemical calculations were performed in the Wrocław Center for Networking and Supercomputing.

■ REFERENCES

(1) Zhang, W.; Moore, J. S. *Angew. Chem., Int. Ed.* **2006**, *45* (27), 4416–4439.
(2) Grave, C.; Schlüter, A. D. *Eur. J. Org. Chem.* **2002**, *2002* (18), 3075–3098.
(3) Iyoda, M.; Yamakawa, J.; Rahman, M. J. *Angew. Chem., Int. Ed.* **2011**, *50* (45), 10522–10553.
(4) Gleiter, R.; Hopf, H. *Modern Cyclophane Chemistry*; John Wiley & Sons: New York, 2006.
(5) Hirst, E. S.; Jasti, R. *J. Org. Chem.* **2012**, *77* (23), 10473–10478.
(6) Omachi, H.; Segawa, Y.; Itami, K. *Acc. Chem. Res.* **2012**, *45* (8), 1378–1389.
(7) Yamago, S.; Kayahara, E.; Iwamoto, T. *Chem. Rec.* **2014**, *14* (1), 84–100.
(8) Gutsche, C. D. *Calixarenes: An Introduction*; Royal Society of Chemistry: London, 2008.
(9) Huang, W.-H.; Zavalij, P. Y.; Isaacs, L. *J. Am. Chem. Soc.* **2008**, *130* (26), 8446–8454.
(10) Xue, M.; Yang, Y.; Chi, X.; Zhang, Z.; Huang, F. *Acc. Chem. Res.* **2012**, *45* (8), 1294–1308.
(11) Schneebeli, S. T.; Cheng, C.; Hartlieb, K. J.; Strutt, N. L.; Sarjeant, A. A.; Stern, C. L.; Stoddart, J. F. *Chem.–Eur. J.* **2013**, *19* (12), 3860–3868.
(12) Lindsey, J. S. *Acc. Chem. Res.* **2010**, *43* (2), 300–311.
(13) Sessler, J. L.; Seidel, D. *Angew. Chem., Int. Ed.* **2003**, *42* (42), 5134–5175.
(14) Li, X.; Upton, T. G.; Gibb, C. L. D.; Gibb, B. C. *J. Am. Chem. Soc.* **2003**, *125* (3), 650–651.
(15) Jung, S.-H.; Pisula, W.; Rouhanipour, A.; Räder, H. J.; Jacob, J.; Müllen, K. *Angew. Chem., Int. Ed.* **2006**, *45* (28), 4685–4690.
(16) Hoffmann, M.; Wilson, C. J.; Odell, B.; Anderson, H. L. *Angew. Chem., Int. Ed.* **2007**, *46* (17), 3122–3125.
(17) Simon, S. C.; Schmaltz, B.; Rouhanipour, A.; Räder, H. J.; Müllen, K. *Adv. Mater.* **2009**, *21* (1), 83–85.

DOI: 10.1021/acs.joc.5b00745
J. Org. Chem. 2015, 80, 6300–6312

(18) Hoffmann, M.; Kärnbratt, J.; Chang, M.-H.; Herz, L. M.; Albinsson, B.; Anderson, H. L. *Angew. Chem., Int. Ed.* **2008**, *47* (27), 4993−4996.
(19) Höger, S. *Pure Appl. Chem.* **2010**, *82* (4), 821−830.
(20) Wang, J.-L.; Li, X.; Lu, X.; Hsieh, I.-F.; Cao, Y.; Moorefield, C. N.; Wesdemiotis, C.; Cheng, S. Z. D.; Newkome, G. R. *J. Am. Chem. Soc.* **2011**, *133* (30), 11450−11453.
(21) O'Sullivan, M. C.; Sprafke, J. K.; Kondratuk, D. V.; Rinfray, C.; Claridge, T. D. W.; Saywell, A.; Blunt, M. O.; O'Shea, J. N.; Beton, P. H.; Malfois, M.; Anderson, H. L. *Nature* **2011**, *469* (7328), 72−75.
(22) Ferguson, J. S.; Yamato, K.; Liu, R.; He, L.; Zeng, X. C.; Gong, B. *Angew. Chem., Int. Ed.* **2009**, *48* (17), 3150−3154.
(23) Feng, W.; Yamato, K.; Yang, L.; Ferguson, J. S.; Zhong, L.; Zou, S.; Yuan, L.; Zeng, X. C.; Gong, B. *J. Am. Chem. Soc.* **2009**, *131* (7), 2629−2637.
(24) Prautzsch, V.; Ibach, S.; Vögtle, F. *J. Incl. Phenom. Macrocycl. Chem.* **1999**, *33* (4), 427−458.
(25) Paioni, R.; Jenny, W. *Helv. Chim. Acta* **1969**, *52* (7), 2041−2054.
(26) Paioni, R.; Jenny, W. *Helv. Chim. Acta* **1970**, *53* (1), 141−154.
(27) Tabushi, I.; Yamada, H.; Kuroda, Y. *J. Org. Chem.* **1975**, *40* (13), 1946−1949.
(28) Shin, J.-Y.; Furuta, H.; Yoza, K.; Igarashi, S.; Osuka, A. *J. Am. Chem. Soc.* **2001**, *123* (29), 7190−7191.
(29) Jacobson, H.; Stockmayer, W. H. *J. Chem. Phys.* **1950**, *18* (12), 1600−1606.
(30) Holler, M.; Allenbach, N.; Sonet, J.; Nierengarten, J.-F. *Chem. Commun.* **2012**, *48* (20), 2576−2578.
(31) Wittig, G.; Geissler, G. *Justus Liebigs Ann. Chem.* **1953**, *580* (1), 44−57.
(32) Maryanoff, B. E.; Reitz, A. B. *Chem. Rev.* **1989**, *89* (4), 863−927.
(33) Byrne, P. A.; Gilheany, D. G. *Chem. Soc. Rev.* **2013**, *42* (16), 6670−6696.
(34) Griffin, C. E.; Martin, K. R.; Douglas, B. E. *J. Org. Chem.* **1962**, *27* (5), 1627−1631.
(35) Elix, J. A. *Chem. Commun. (London)* **1968**, *6*, 343−344.
(36) Brown, C.; Sargent, M. V. *J. Chem. Soc. C* **1969**, *13*, 1818−1820.
(37) Tulloch, C. D.; Kemp, W. *J. Chem. Soc., Chem. Commun.* **1971**, *14*, 747a−747a.
(38) Thulin, B.; Wennerström, O.; Hogberg, H. E. *Acta Chem. Scand. Ser. B* **1975**, *B29* (1), 138−139.
(39) Hoegberg, H. E.; Thulin, B.; Wennerström, O. *Tetrahedron Lett.* **1977**, *11*, 931−934.
(40) Strand, A.; Thulin, B.; Wennerström, O. *Acta Chem. Scand. Ser. B* **1977**, *B31* (6), 521−523.
(41) Thulin, B.; Wennerström, O.; Somfai, I.; Chmielarz, B. *Acta Chem. Scand. Ser. B* **1977**, *B31* (2), 135−140.
(42) Thulin, B.; Wennerström, O.; Somfai, I. *Acta Chem. Scand. Ser. B* **1978**, *B32* (2), 109−117.
(43) Tanner, D.; Wennerström, O. *Acta Chem. Scand. Ser. B* **1980**, *B34* (7), 529−535.
(44) Hoegberg, H.-E.; Wennerström, O. *Acta Chem. Scand. Ser. B* **1982**, *B36* (10), 661−667.
(45) Raston, I.; Wennerström, O. *Acta Chem. Scand. Ser. B* **1982**, *B36* (10), 655−660.
(46) Tanner, D.; Wennerström, O. *Acta Chem. Scand. Ser. B* **1983**, *B37* (8), 693−698.
(47) Tihulin, B.; Wennerström, O. *Acta Chem. Scand. Ser. B* **1983**, *B37* (4), 297−301.
(48) Wennerström, O.; Raston, I.; Sundahl, M.; Tanner, D. *Chem. Scr.* **1987**, *27* (4), 567−568.
(49) Vogtle, F.; Hochberg, R.; Kochendörfer, F.; Windscheif, P.-M.; Volkmann, M.; Jansenb, M. *Chem. Ber.* **1990**, *123* (11), 2181−2185.
(50) Märkl, G.; Knott, T.; Kreitmeier, P.; Burgemeister, T.; Kastner, F. *Helv. Chim. Acta* **1998**, *81* (5−8), 1480−1505.
(51) Märkl, G.; Ehrl, R.; Sauer, H.; Kreitmeier, P.; Burgemeister, T. *Helv. Chim. Acta* **1999**, *82* (1), 59−84.
(52) Märkl, G.; Ehrl, R.; Kreitmeier, P.; Burgemeister, T. *Helv. Chim. Acta* **2000**, *83* (2), 495−511.
(53) Wandel, H.; Wiest, O. *J. Org. Chem.* **2001**, *67* (2), 388−393.
(54) Rieger, R.; Kastler, M.; Enkelmann, V.; Müllen, K. *Chem.−Eur. J.* **2008**, *14* (21), 6322−6325.
(55) Esser, B.; Bandyopadhyay, A.; Rominger, F.; Gleiter, R. *Chem.−Eur. J.* **2009**, *15* (14), 3368−3379.
(56) Harrowven, D. C.; Kostiuk, S. L. *Nat. Prod. Rep.* **2012**, *29* (2), 223−242.
(57) McDonald, R. N.; Campbell, T. W. *J. Org. Chem.* **1959**, *24* (12), 1969−1975.
(58) Siegel, B. *J. Am. Chem. Soc.* **1979**, *101* (9), 2265−2268.
(59) Ngwendson, J. N.; Schultze, C. M.; Bollinger, J. W.; Banerjee, A. *Can. J. Chem.* **2008**, *86* (7), 668−675.
(60) Yamataka, H.; Nagareda, K.; Ando, K.; Hanafusa, T. *J. Org. Chem.* **1992**, *57* (10), 2865−2869.
(61) Hwang, J.-J.; Lin, R.-L.; Shieh, R.-L.; Jwo, J.-J. *J. Mol. Catal. Chem.* **1999**, *142* (2), 125−139.
(62) Dunne, E. C.; Coyne, É. J.; Crowley, P. B.; Gilheany, D. G. *Tetrahedron Lett.* **2002**, *43* (13), 2449−2453.
(63) Byrne, P. A.; Gilheany, D. G. *J. Am. Chem. Soc.* **2012**, *134* (22), 9225−9239.
(64) Stępień, M. *J. Org. Chem.* **2013**, *78* (18), 9512−9516.
(65) Myśliwiec, D.; Stępień, M. *Angew. Chem., Int. Ed.* **2013**, *52* (6), 1713−1717.
(66) Stępień, M. *Synlett* **2013**, *24* (11), 1316−1321.
(67) Robiette, R.; Richardson, J.; Aggarwal, V. K.; Harvey, J. N. *J. Am. Chem. Soc.* **2005**, *127* (39), 13468−13469.
(68) Robiette, R.; Richardson, J.; Aggarwal, V. K.; Harvey, J. N. *J. Am. Chem. Soc.* **2006**, *128* (7), 2394−2409.
(69) Harvey, J. N. *Faraday Discuss.* **2010**, *145* (0), 487−505.
(70) Speziale, A. J.; Bissing, D. E. *J. Am. Chem. Soc.* **1963**, *85* (23), 3878−3884.
(71) Yamataka, H.; Nagareda, K.; Takatsuka, T.; Ando, K.; Hanafusa, T.; Nagase, S. *J. Am. Chem. Soc.* **1993**, *115* (19), 8570−8576.
(72) Ercolani, G.; Mandolini, L.; Mencarelli, P. *Macromolecules* **1988**, *21* (5), 1241−1246.
(73) Wu, F.-I.; Shih, P.-I.; Yuan, M.-C.; Dixit, A. K.; Shu, C.-F.; Chung, Z.-M.; Diau, E. W.-G. *J. Mater. Chem.* **2005**, *15* (44), 4753.
(74) Scalmani, G.; Frisch, M. J. *J. Chem. Phys.* **2010**, *132* (11), 114110.
(75) Tomasi, J.; Mennucci, B.; Cammi, R. *Chem. Rev.* **2005**, *105* (8), 2999−3094.
(76) Sheldrick, G. M. *Acta Crystallogr., Sect. A: Found. Crystallogr.* **2008**, *64* (1), 112−122.
(77) Clark, R. C.; Reid, J. S. *Acta Crystallogr., Sect. A: Found. Crystallogr.* **1995**, *51* (6), 887−897.

DOI: 10.1021/acs.joc.5b00745
J. Org. Chem. 2015, 80, 6300−6312